1985

Modeling of the settling of thick slurries

Gregory J. Hanson
Iowa State University

Hanson, Gregory J.

MODELING OF THE SETTLING OF THICK SLURRIES

Iowa State University PH.D. 1985

Modeling of the settling of thick slurries

by

Gregory J. Hanson

A Dissertation Submitted to the

Graduate Faculty in Partial Fulfillment of the

Requirements for the Degree of

DOCTOR OF PHILOSOPHY

Department: Civil Engineering
Major: Geotechnical Engineering

Approved:

Signature was redacted for privacy.

In Charge of Major Work

Signature was redacted for privacy.

For the Major Department

Signature was redacted for privacy.

For the Graduate College

Iowa State University
Ames, Iowa

1985

TABLE OF CONTENTS

GENERAL INTRODUCTION

The settling of solids through a fluid is of concern to many fields of engineering including sanitary, mining, chemical, and geotechnical. The settling process of a slurry can be classified into four categories: 1) discrete settling in which the particles behave as individual units, 2) flocculent settling in which individual particles agglomerate to form larger units, 3) zone settling in which flocs come together to form a three dimensional matrix, and 4) consolidation which occurs when the slurry has reached a very high concentration. In order to design a solid-liquid separation system, whether it be a dredge containment site or a thickener, it is necessary to observe the settling characteristics of the slurry and to predict the time rate of settlement and the amount that the slurry will consolidate over the long term. The observations are usually conducted in a settling column in the laboratory and various approaches have been used to analyze the observations.

This dissertation is composed of four parts which discusses three topics involved in the study of solid-liquid separation: 1) extension of the large strain consolidation theory to evaluate the time rate of settling, 2) comparison of three models for predicting the magnitude of consolidation with actual measurements of consolidation at the Panorama dredge spoil site, and 3) conceptual design of an instrument for measuring the consolidation behavior of slurries.

Parts I and II - "Hypothesis of settling phenomenon" and "Hypothesis of settling phenomenon: numerical evidence" discuss the first topic. The large strain consolidation theory is formulated in

terms of an advection-diffusion equation and the interface versus time curves from settling tests are interpreted such that a metastable structure forms when an interface forms in the slurry. The diffusion portion of the equation is dominant during this phase of the process until the structure collapses. As the structure collapses, the advection term becomes important, until the process once again slows down. In the final phase, diffusion is the important term in the equation. This model was modified from previous models by using Poiseuille's law to describe the relationship between permeability and density of the slurry. The model was tested numerically with a finite element solution in comparison with published data.

Part III - "Predicting settlement for extended periods of time" discusses the second topic. Three methods of estimating the long term volume change that a slurry will experience are evaluated by comparing the predictions of laboratory tests with field observations at the Lake Panorama dredge slurry disposal site.

Part IV - "Electrical properties of slurries" discusses the third topic of study. The need for a more economical method of determininig the density variations within slurries in a settling column led to an investigation of the electrical properties of slurries. This study involved measuring electrical properties of three different slurries including the Lake Panorama sediment.

PART I. HYPOTHESIS OF SETTLING PHENOMENON

INTRODUCTION

Since the work carried out by Coe and Clevenger (1916), there have been a number of models proposed for describing the settling process of a slurry. Gaudin et al. (1959) reasoned that there were two principal attributes of a slurry that should be determined. The first attribute being the settling rate and the second being the ultimate slurry density. These two attributes have been the focus of most modeling of slurry settling. The objectives of this paper are to review the observations and models that have been derived for describing the settling process and to present an improved hypothesis and model for the description of the settling process.

OBSERVATIONS OF THE SETTLING PROCESS - AN OVERVIEW

The settling behavior of slurries is commonly classified into four categories based on the degree of solids concentration and interparticle cohesiveness:

1. Discrete particle settling: This occurs when particles settle as individual entities, and there is no significant interaction with neighboring particles. This type of settling occurs in slurries of low solids concentration.

2. Flocculent settling: This occurs when solids concentrations are low and particles have a high tendency towards agglomeration. Individual flocs form increasing their mass and thereby increase the rate of settling over that of individual particles.

3. Zone settling (also called hindered settling): This occurs in slurries of intermediate concentrations, in which interparticle forces are sufficient to hinder the settling of neighboring particles. The particles tend to remain in fixed positions relative to each other, and the mass of particles settles as a unit. A solids-liquid interface develops at the top of the settling mass.

4. Compression settling: This occurs in slurries of high concentrations in which a structure has formed, and further settling occurs by compression of the structure. Compression of the structure is caused by increased weight due to the particles which are constantly being added by the sedimentation process.

The primary focus of this overview and this paper will be on slurries in which an interface has formed. As previously noted, interface formation is an indication of zone settling. Due to the physical chemical variability of slurries, tests on specific slurries are required to characterize their settling behavior. Typical settling tests involve observing the settling of the interface that forms between the region of zone settling and the zone of clear water above. The time versus interface descent curve from a settling test is shown in Figure 1. The

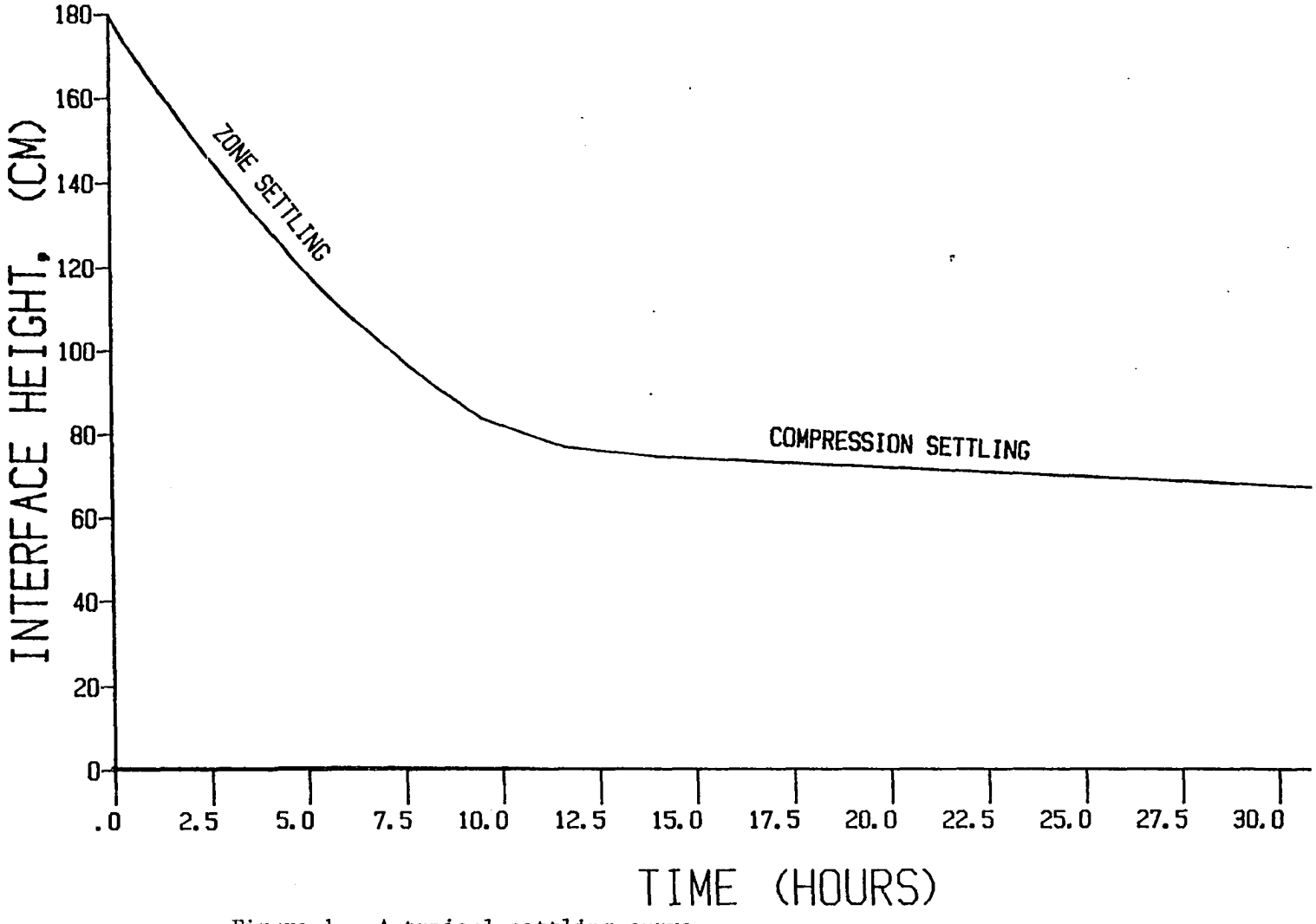

Figure 1. A typical settling curve

early portion is commonly referred to as zone or hindered settling. Whereas, the latter portion is referred to as compression settling. A typical settling curve is generally depicted as having a linear descent before the transition to compression settling, but this is not always the case. Figures 2 and 3 show settling tests in which initial settling is not necessarily linear. Settling tests in which initial settling is linear have been labeled "ideal settling tests." As the initial slurry concentration increases, the nonlinearity or delay in settling, also increases. It has also been observed that the interface settling velocity increases with increased initial depth of slurry (Gaudin et al., 1959; Micheals and Bolger, 1962; Dick and Ewing, 1967).

Below this interface there are considered to be three zones; the zone of constant concentration, the transition zone with concentration increasing from top to bottom, and the compression zone where further elimination of water is a function of time. As the settling tests continue, the zone of constant concentration and the transition zone disappear and the whole system undergoes compression settling, and eventually settling stops altogether. It is clear that during the period designated as zone settling both zone settling and compression settling are occurring. The compression settling region initially begins at the bottom and as settling continues the entire slurry has entered compression settling. It is presumed that the reason for the zone settling designation is that zone settling is dominating the rate of interface descent in the early period of settling.

Based on observations of kaolinite slurries, Gaudin and Fuerstenau

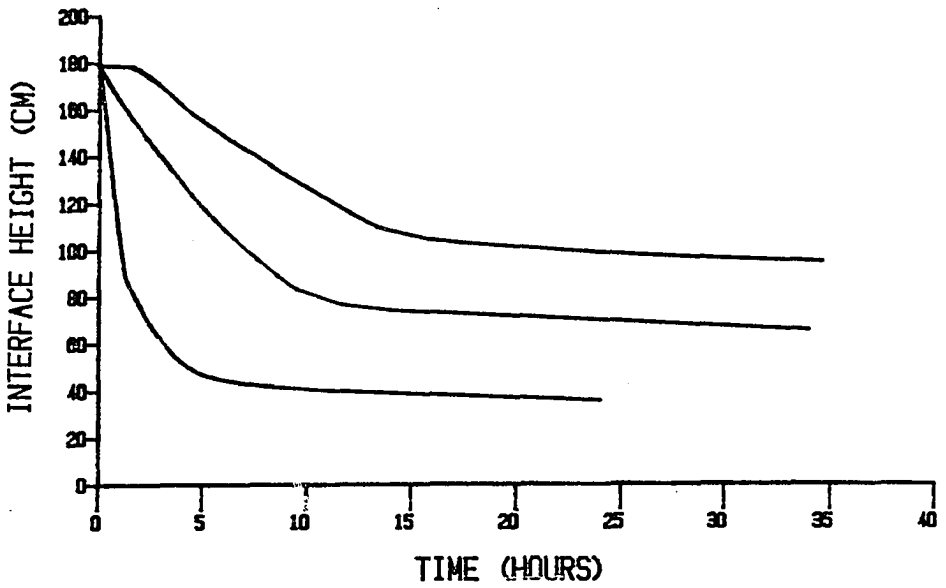

Figure 2. Settling curves from study by Lin (1983)

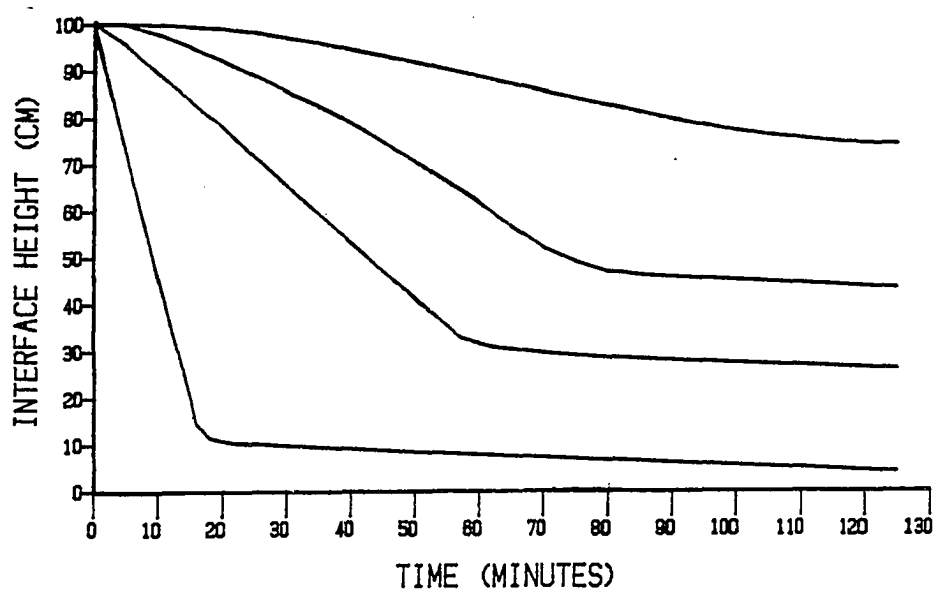

Figure 3. Settling curves from study by Fuerstenau (1960)

(1962) concluded that the observation of the slurry interface descent may actually be misleading to understanding the settling process. Therefore, they developed an x-ray transviewer capable of evaluating the slurry density at various times and positions. Figure 4 shows that a density step forms at the bottom of the column and propagates upwards with time. It can be observed that the density step forms, propagates upwards to the interface, and once it reaches the interface disappears. At this point in time, the interface descent slows down entering compression settling. It should also be noted that the slurry density at the bottom of the column continues to increase with time.

Been and Sills (1981) also developed an x-ray transviewer to observe density changes in a typical estuarine mud. Their results were similar to Gaudin and Fuerstenau (1962) in that they also observed the density step phenomenon. In addition, they observed that if the initial slurry concentration was increased to a certain level, a density step did not form during the entire settling process. It was also observed by Been and Sills (1981) that a high density layer formed at the base of the column during settling tests. Been and Sills (1981) attributed this high density layer to differential settling in which the larger particles were not held in suspension and settled out rapidly. This layer was not observed in higher concentration slurries and they attributed this to the stronger structure inhibiting differential settlement.

Channeling is also an important phenomenon which plays a role in the settling process (Gaudin and Fuerstenau, 1962; Been, 1980; Dell and Kaynar, 1968; Vesilind, 1979). Gaudin and Fuerstenau (1962) observed two types

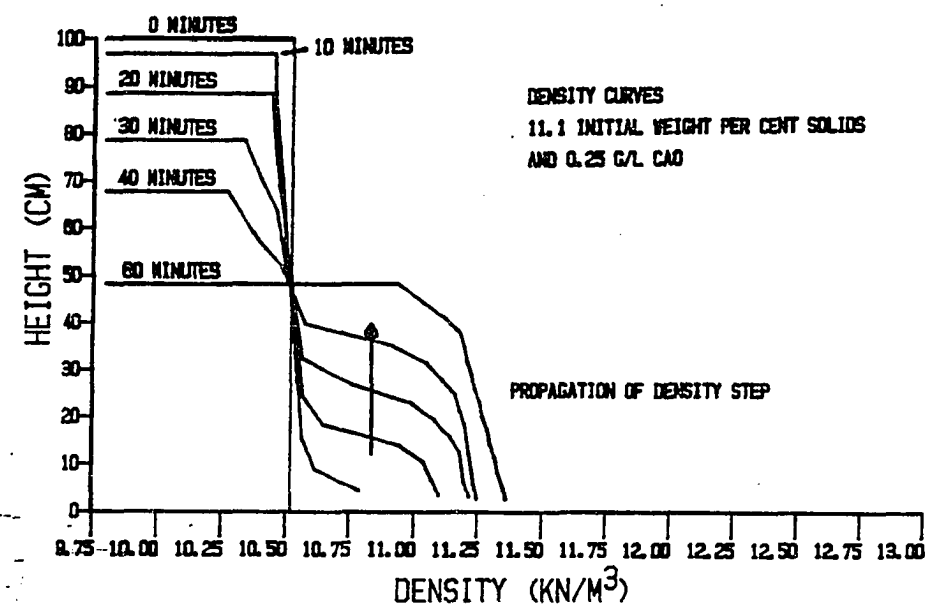

Figure 4. Density profiles with depth and time (Fuerstenau, 1960)

of flow patterns in the settling of relatively thick slurries and referred to them as tube flow (channeling) and tubule flow. The tubes are large channels and the tubules are minute pores. Flow tubes occur early in the sedimentation process, whereas flow through tubules occurs throughout the entire sedimentation process. While the tubes exist, they carry almost all of the flow. Dell and Kaynar (1968) observed that the zone of channeling was fairly sharp. It was observed to propagate from the bottom upward. Increased flocculant dosage appeared to decrease the rate of rise of the channeled zone; and at the highest dosage no large channels were observed at all. When channels were observed, it was noted that they would reach the slurry interface at approximately the same time the interface descent curve was observed to flatten out. The observation of channel propagation through the slurry resembles that of the density step propagation. When channels reach the interface, Been (1980) described them as volcanoes erupting.

These observations along with the few observations of particle-particle interactions have led to theories of the phenomenological process involved in settling. The basic unit involved in flocculent sedimentation is generally accepted to be small clusters of particles plus enclosed water called flocs. Michaels and Bolger (1962) observed, using a 45x microscope mounted against the glass tube wall, that in dilute concentrations these flocs were attached in clusters called aggregates. In dilute suspensions, these aggregates were observed to settle as roughly spherical individual units. Michaels and Bolger (1962) proposed that in thicker concentrations these aggregates formed extended

networks which give the suspension its plastic and structural properties.

There are two schools of thought as to why an interface forms. The one proposed by Michaels and Bolger (1962) is that if the aggregates are of the same size and density, they will settle at the same rate giving a sharp clear interface. Whereas, aggregates of varied size will give a cloudy supernatant. The second school of thought is that the existence of a clear interface in a flocculent slurry is due to the particles being held in the same relative position in a continuous lattice (Lawler et al., 1982; Lin and Lohnes, 1984). Been (1980) noted that an interface does not form in a slurry which has been treated with a dispersing agent.

The phenomenological process involved in zone settling has also been interpreted in primarily two ways. The first interpretation is that the settling process is a purely fluid-particle interaction phenomenon. As the particle concentration increases, the particles will begin to restrict the area through which the displaced fluid may flow upward. The velocity of the fluid therefore increases, creating greater drag resistance therefore causing the particles to settle at a lower velocity. The second interpretation of the zone settling process is that particle-particle interaction plays an important role as well as fluid-particle interaction. Dick and Ewing (1967) stated that:

> "Furthermore, and possibly of most importance, it seems likely that a network of aggregate particles could form a structural suspension exhibiting a yield strength. The existence of such a structure would permit interparticle forces."

Figure 5 shows the proposed fabric of aggregate networks proposed by Michaels and Bolger (1962). Fuerstenau (1960) went so far as to say that

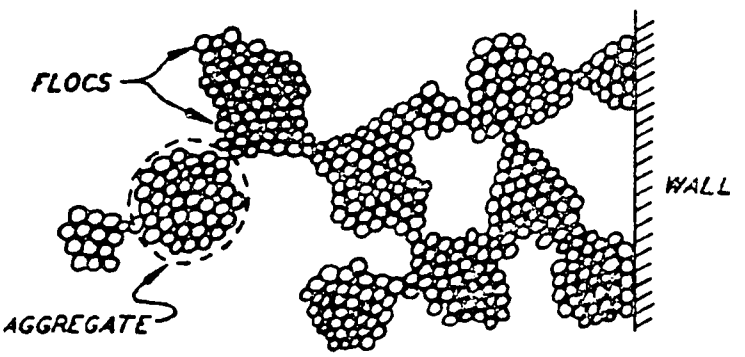

Figure 5. Floc-aggregate structural model (Michaels and Bolger, 1962)

the settling of thick slurries was just two phases of compression, competent compression settling and incompetent compression settling. The slurry forms as one large floc and competent settling occurs early on where water escapes easily due to the existence of tube flow. Incompetent compression settling occurs in the latter portion of settling when water escapes with more difficulty due to tubule flow.

MODELING SLURRY SETTLING - AN OVERVIEW

The purpose of this portion is to present the direction that modeling has taken and also as a preparation for the model to be proposed in this paper. Both of the phenomenological interpretations, presented in the previous section, of the settling process have been used for modeling purposes. Four models have been reviewed. Two models have focused on modeling based on particle-fluid interaction (Kynch, 1952; Yong and Elmonayeri, 1984). The two other models have focused on the particle-particle interaction as well as particle fluid interaction (Been and Sills, 1981; Lin and Lohnes, 1984).

Kynch (1952) proposed a theory of sedimentation based primarily on the mathematics of kinematic waves. The theory assumes that the velocity of fall, v, of particles is determined by the local concentration, c, of particles only and the relationship between the two can be determined by the observations of the interface descent. The settling process is then determined entirely from a consideration of continuity without knowing the details of particle interaction. The general equation may be expressed as follows:

$$\frac{\partial c}{\partial t} + V(c)\frac{\partial c}{\partial x} = 0 \quad . \tag{1}$$

V(c) is a velocity in which V(c)=-ds/dc, where s is the particle flux, the number of particles crossing a horizontal section per unit area per unit of time, or s=cv. This theory states that during the settling process the concentration increases near the bottom and propagates upward as a discontinuity, with a velocity V(c). The (c) indicates that the

propagation velocity of the discontinuity is concentration dependent. Kynch (1952) also assumed that the maximum density is obtained at the bottom of the settling test at time=0. When this density discontinuity propagates to the top of the sediment, the settling stops. Kynch's theory predicts a linear falling interface for early portions of the settling test. The interface descent however, as previously stated, has been observed to be strongly nonlinear even in the early stages of settling tests (Gaudin et al., 1959; Fitch, 1962; Been, 1980; Lin, 1983). The Kynch theory is adequate for predicting the settling process of particles where there is little particle interaction (i.e., sands or dilute concentrations of clays). As concentrations of solids tend to zero, the Kynch model reduces to Stoke's theory (Schiffman et al., 1984).

The Kynch model was an important contribution to the modeling of the settling process but is a model with little physical basis. Kynch's theory became popular because it implied that the settling velocity was a function of concentration only. Therefore, thickener designs could be based on a single settling test.

Been (1980) observed the settling process of natural bay sediments using an x-ray transviewer. He concluded that thicker slurries and slurries in which the zone of constant concentration and the transition zone have disappeared could be modeled by simplification of the large strain consolidation equation formulated by Gibson et al. (1967). The large strain consolidation equation may be written in the following form:

$$\frac{\partial e}{\partial t} = -\frac{\partial}{\partial z}\left(\frac{K(e)}{\rho_f(1+e)}\frac{d\sigma'}{de}\frac{\partial e}{\partial z}\right) - \left(\frac{\rho_s}{\rho_f} - 1\right)\frac{d}{de}\left(\frac{K(e)}{(1+e)}\right)\frac{\partial e}{\partial z} \qquad (2)$$

ρ_s and ρ_f are the density of the solid and fluid, respectively. The void ratio, e, is the volume of voids divided by the volume of solids. The permeability, K(e), of the soil is a function of the void ratio. The effective stress, σ', which is defined as the total stress minus the pore pressure. z is a material coordinate where $x = \int_0^z (1+e)dz$.

Gibson et al. (1967) derived this equation because of the shortcomings of the simplifying assumptions used in Terzaghi's widely recognized theory of one dimensional consolidation. In the large strain consolidation equation, parameters are considered to vary, void ratio is not necessarily uniform throughout the sample thickness and the validity of Darcy's law has been assumed but is recast in a form that relates the relative velocities of the soil and pore fluid to the excess pore pressure gradient. Furthermore, the limitation of fixed soil boundaries as prescribed in conventional consolidation theory is removed. The use of the material coordinate system is convenient for describing the consolidation behavior. While the boundary moves in the conventional space coordinate system, the boundary does not move in the material coordinate system.

In order to solve the equation analytically, Lee and Sills (1981), assumed that:

(1) The void ratio versus effective stress is a linear relationship;

$$\sigma' = A - \alpha e \qquad (3)$$

where A and α are constant.

(2) The permeability versus void ratio is a linear relationship;

$$K(e) = \rho_f K_0 (1+e) \tag{4}$$

where K_0 is a constant, and

(3) The coefficient of consolidation C_F is a constant where

$$C_F = - \frac{K(e)}{\rho_f (1+e)} \cdot \frac{d\sigma'}{de} \tag{5}$$

By applying the assumptions given by Equations (3), (4), and (5), Equation (2) reduces to the following form:

$$\frac{\partial e}{\partial t} = C_F \frac{\partial^2 e}{\partial z^2} \tag{6}$$

Been and Sills (1981) used Equation (6) as the basis for their model of compression settling. Been and Sills (1981) altered the analytical approach to this equation in order to compensate for observed void ratio changes at the interface during a settling test. In summary, the Lee and Sills (1981) approach assumed that the void ratio at the surface of a soil deposit would not change during consolidation. Been and Sills (1981) observed that during compression settling the void ratio at the surface continued to decrease with time therefore an adjustment in the approach was required. For a more detailed description of the Lee and Sills (1981) approach versus that of Been and Sills (1981), see Lin (1983).

Lin (1983) concluded from his work, that the self-weight consolidation model of Been and Sills (1981) could be used in modeling the

entire settling process of a slurry in which an interface has formed. Lin (1983) observed, and was supported by the observations of Gaudin and Fuerstenau (1962), and Michaels and Bolger (1962) that after an interface has formed there is no jockeying for position by the particles. The slurry settles as if the particles are locked into an interconnected lattice. Therefore, effective stresses are existent and the structure begins to consolidate under its own weight. Hence, Lin (1983) concluded that the Been and Sills (1981) approach could be applied to zone settling as well. This approach has the advantage of clearly defining the beginning point at which the model may be applied. Lin (1983) also developed methodologies for determining the critical concentration, that concentration at which an interface forms, and in turn the beginning of the self-weight consolidation model.

The self-weight consolidation equation of Lee and Sills (1981) and Terzaghi's conventional consolidation equation are commonly termed "diffusion equations." A recent development in the modeling of the settling process is the advection-diffusion equation by Yong and Elmonayeri (1984). They have suggested a method of analysis which addresses the solids concentration range covered by discrete settling and hindered settling. Whereas, the self-weight consolidation model can be used to analyze the solids concentration range covered by compression settling. Yong and Elmonayeri (1984) suggest that these two models define subgroups of the settling process and that combined they are capable of describing the entire settling process. Yong and Elmonayeri (1984) compared their model with interface descent curves.

Yong and Elmonayeri's (1984) advection-diffusion equation is based on the modeling of relative fluxes. These fluxes consist of a fluid flux (q_f) and a solids flux (q_s). The resultant fluid flux consists of a flux of fluid moving upwards (q_{fs}) relative to the downward moving solids (q_s) and a portion of the fluid associated with the convective solids (βq_s). Yong and Elmonayeri (1984) have expressed this relationship in the following manner:

$$q_f = q_{fs} + \beta q_s \tag{7}$$

The continuity condition considering movement in one dimension is the following:

$$-\frac{\partial \alpha}{\partial t} = \frac{\partial q_f}{\partial \xi} = \frac{\partial q_{fs}}{\partial \xi} + \frac{\partial (\beta q_s)}{\partial \xi} \tag{8}$$

Where ξ is the upward positive spatial coordinate with the origin of the axis at the base (see Figure 6). $\alpha = \alpha_d + \alpha_{cv}$ is the total amount of fluid that appears above the solids liquid interface. α_d is the volumetric content of fluid released due to diffusive flow and α_{cv} is the volumetric content of fluid lost due to convective flow.

The internal driving forces result in potential differences which cause an upward flux of fluids past the solids (Yong and Elmonayeri, 1984). The final form of their equation is as follows:

$$\frac{\partial \alpha}{\partial t} = \frac{\partial}{\partial \xi}\left(D \frac{\partial \alpha_d}{\partial \xi} \right) - \beta \frac{\partial q_s}{\partial \xi} - q_s \frac{\partial \beta}{\partial \xi} \tag{9}$$

where

D = a diffusion constant.

This is the governing relationship given by Yong and Elmonayeri (1984). Yong and Elmonayeri's (1984) governing relationship is based primarily on fluxes and they indicated that it must be critically examined when interparticle contact becomes a significant issue.

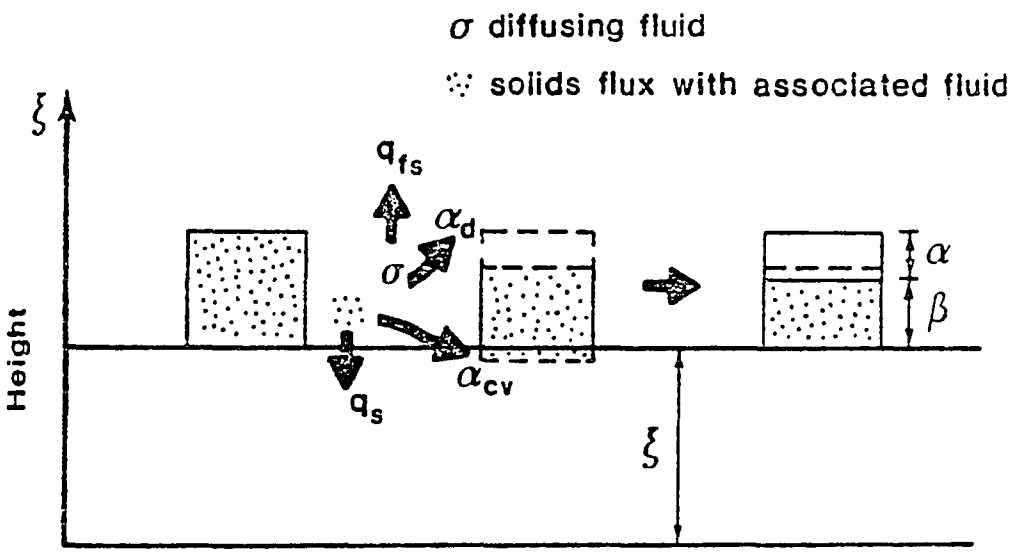

Figure 6. Schematic representation of developed fluxes in a control volume, showing fluid flux relative to solids q_{fs} flowing in the upward side direction, and q_s solids flux leaving the control volume with associated fluid $q_s = \alpha_{cv}$ (Yong and Elmonyeri, 1984)

HYPOTHESIS OF PHENOMENOLOGICAL PROCESS AND RATIONALE

The delay in settling which occurs early in the settling history of some slurries has been observed to become greater in tests with greater initial solids concentration. Gaudin et al. (1959) referred to this as an inductive time for flocculation but this does not seem to be an appropriate explanation because of the increased delay with increased concentration. This delay in settling appears to be an important aspect in the settling process, on par with the transition from zone settling to compression settling. In tests of lower concentration, the initial interface descent is linear as would be anticipated by the Kynch model; but if the solids concentration is increased, a delay period occurs prior to increased rate of settling. Finally, at high solids concentrations, the slurry settling test remains in delayed settling.

It is hypothesized that this phenomenon may be explained by an analogy with soils commonly called "sensitive clays." Normally consolidated soils typically have an effective stress versus void ratio relationship as shown in Figure 7. Whereas, sensitive clays show a relationship similar to Figure 8. The curve in Figure 8 has an almost vertical slope at an effective stress close to a critical stress, σ'_c, indicating that the structure collapses when the pressure is increased beyond σ'_c. Accompanying this breakdown is a dramatic change in void ratio.

Some sensitive clays have their origin as alluvial soils which were deposited in a flocculated fabric. Mitchell (1976) describes the fabric of sensitive clays as follows:

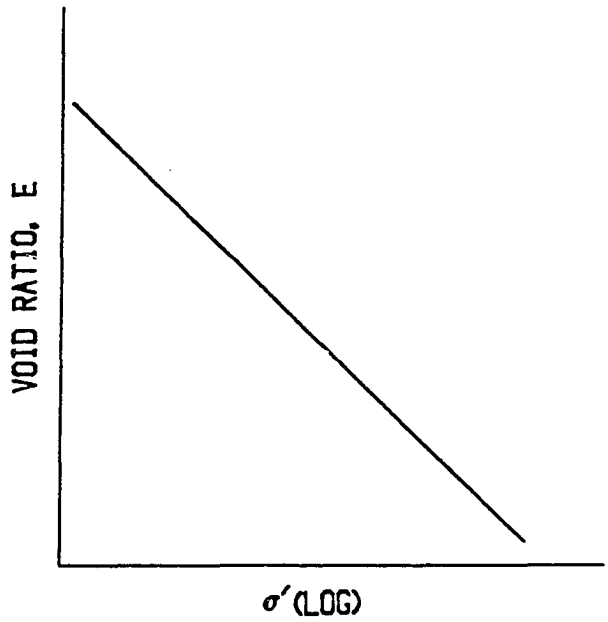

Figure 7. Normally consolidated soil

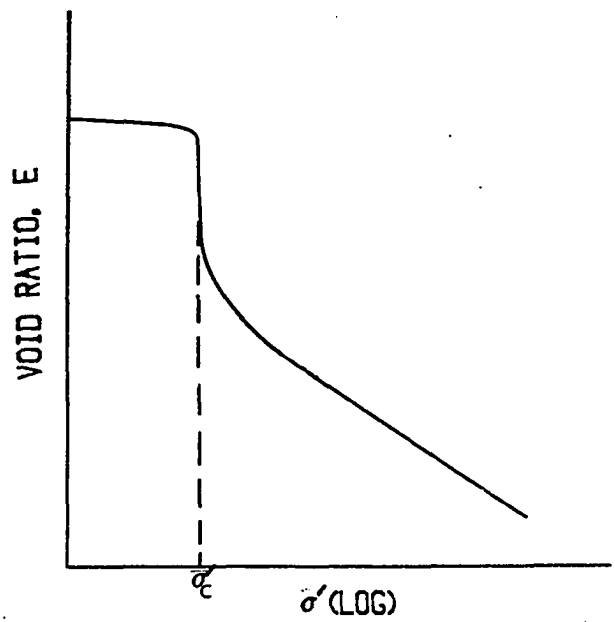

Figure 8. Sensitive clay

> The undisturbed fabric of sensitive clays is composed of flocculated assemblages of particle aggregates. Electron photomicrographs show bookhouse and stepped-flocculated particles arrangements in medium sensitive to quick clays. Very sensitive to quick clays contain irrequlars aggregations linked by connector assemblages which are evidently not common in soils of low to medium sensitivity. Inter-assemblage pores are larger in the clays of high sensitivity than in the more insensitive clays. The contribution of fabric to high sensitivity is through the open networks of irregular aggregation assemblages, linked by unstable connectors.

Figure 9 is a schematic of the sensitive clay fabric and is similar to the structure proposed by Michaels and Bolger (1962) shown in Figure 5.

It is hypothesized that this same type of structure exists in slurry settling where an interface has formed. As a suspension is prepared it is initially at a uniform concentration from top to bottom. The particles flocculate forming a fabric of flocculated assemblages of particle aggregates linked together by networks of connector assemblages. The structure of the slurry is metastable in nature. The stability of the structure is dependent upon the solids concentration, the particle electrical activity, the temperature, and the electrolyte concentration of the solution. As settling begins, all regions of the slurry have a metastable structure which begins to settle due to the weight of the lattice. The stress and strain of this structure is the greatest at the bottom. Therefore, transition to a critical state at which collapse occurs begins at the bottom. This transition may be instantaneous with no visible time lapse before collapse or the transition may require considerable time before collapse. Once collapse occurs a density change also occurs, which in turn creates excess fluid.

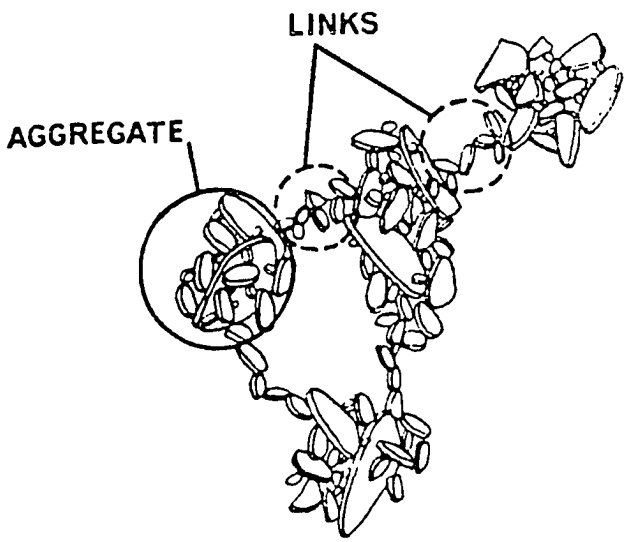

Figure 9. Schematic picture of natural microstructural pattern in the investigated quick clay (Pusch, 1970)

This fluid escapes through weaknesses in the structure above it and therefore, channeling occurs. At this point in time, the observer would note an increased rate of settling at the interface. The density step is formed and propagates upwards in unison with channeling, reaching the interface at approximately the same time, indicating that all the material has been transformed, to a new fabric arrangement.

MODEL

Yong and Elmonayeri (1984) suggest that their model and Been and Sills' (1981) model are models which, when used together, can be used to describe the entire settling process. It is suggested here that it would be more convenient to have a general model capable of describing the entire settling process. The original equation derived by Gibson et al. (1967) may be the basis for accomplishing this task. The equation is similar in form to the conventional "advection-diffusion" equation. It is also based on the physical processes involved in the interaction of fluids and particles (the advection term) and particle interaction, effective stresses and excess pore pressures (the diffusion term). Been (1980) has already shown that when dealing with discrete settling the effective stresses are zero and the large strain consolidation equation becomes equivalent to Kynch's theory which is a purely advective expression. Effective stress is the portion of the total stress carried by the particle structure and the pore pressure is that portion of the total stress carried by the fluid in the space between particles. In discrete settling and flocculent settling, there is no structure formed and therefore, no effective stress. It is then a purely advective phenomenon of gravity and drag resistance.

Been and Sills (1981) have also shown that with certain simplifying assumptions, the large strain consolidation equation can be reduced to a diffusion equation for the purposes of modeling compression settling. The hypothesis presented here is that the equation derived by Gibson et al. (1967) may be used to describe the entire settling process. This

hypothesis seems quite plausible when it is considered that simplifications of the model have been shown to describe the two extremes of the settling phenomenon.

Lin (1983) suggested that the Been and Sills model could be extended on into zone settling. He made this conclusion based on a number of factors. The descent of the interface is not necessarily linear as would be suggested by the Kynch model but rather, in many cases, shows a delay before beginning to descend. Below the interface, there is no jockeying for position by the particles. The particles appear to form one large floc; a three-dimensional lattice. Therefore, interparticle contacts exist and intuitively effective stresses are present as well.

From these observations, Lin (1983) concluded that the consolidation begins at the time the interface is formed. Therefore, he also concluded that the approach suggested by Been and Sills (1981) is applicable for all cases of slurry settling in which a interface has formed. The conclusion that effective stresses exist in the zone settling seems reasonable, but to conclude that the analytical approach presented by Been and Sills (1981) is applicable does not. In the slurry settling tests carried out by Been (1980) and Fuerstenau (1960), they observed the formation of a density step or discontinuity below the interface. Whitham (1974) states that the diffusion term in an equation such as the heat equation has the tendency towards smoothing out a density step; therefore, not having the capability of modeling phenomenon in which one occurs. Whereas, the advection term has the tendency towards steepening

and breaking therefore causing a step to occur. The large strain consolidation equation has the two opposite tendencies combined in one equation.

A model using the large strain consolidation equation would be capable of describing the change in effective stresses and permeability that have been described in the hypothesis of zone and compression settling. Figure 10 indicates the phases of a settling test which has visible delay in settling. The initial period is under compression settling or consolidation. Following that, zone settling occurs due to the collapse of the structure and a density step forms. At the time of collapse, three distinct zones form, the zone of constant concentration, the zone of transition, and the zone of compression. Figure 10 idealizes the transition zone as a line representing the boundary between zone settling and compression settling. This line represents the average rate and direction of propagation of the density step.

Figure 11 is a schematic of the density changes with time. For the initial phase, $0 < t < t_1$, compression settling is occurring. For $t_1 < t < t_2$, zone settling and compression settling are occurring with a transition zone between, in which collapse and reformation are occurring. Eventually for $t_2 < t$, the entire slurry is in compression settling.

The proposed structural changes that occur during the settling process are shown in Figure 12. For the initial phase, $0 < t < t_1$, the fabric is a combination of links and aggregates. The aggregates are becoming closer at the bottom, but the fabric still has integrity and

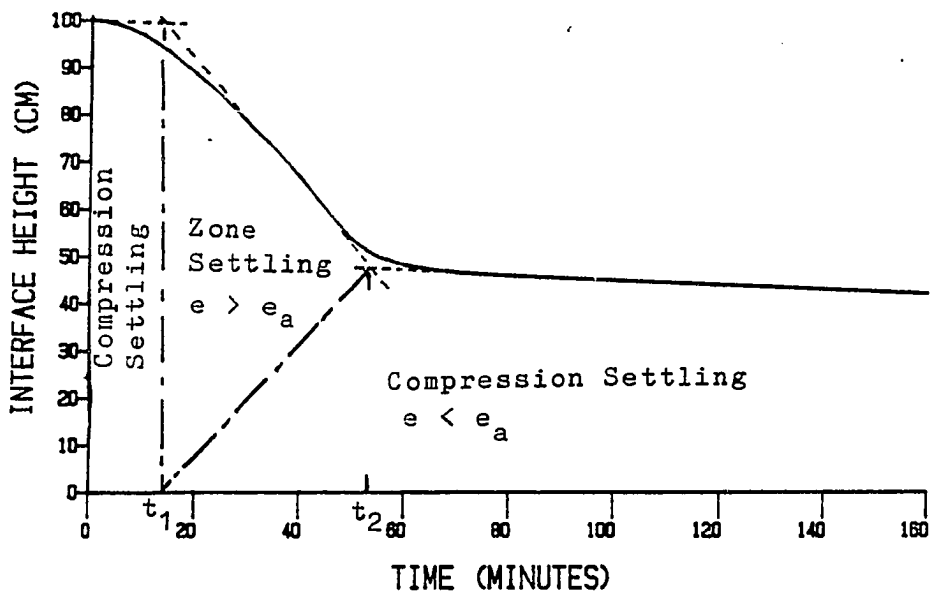

Figure 10. Phases of reverse "S" shaped settling test

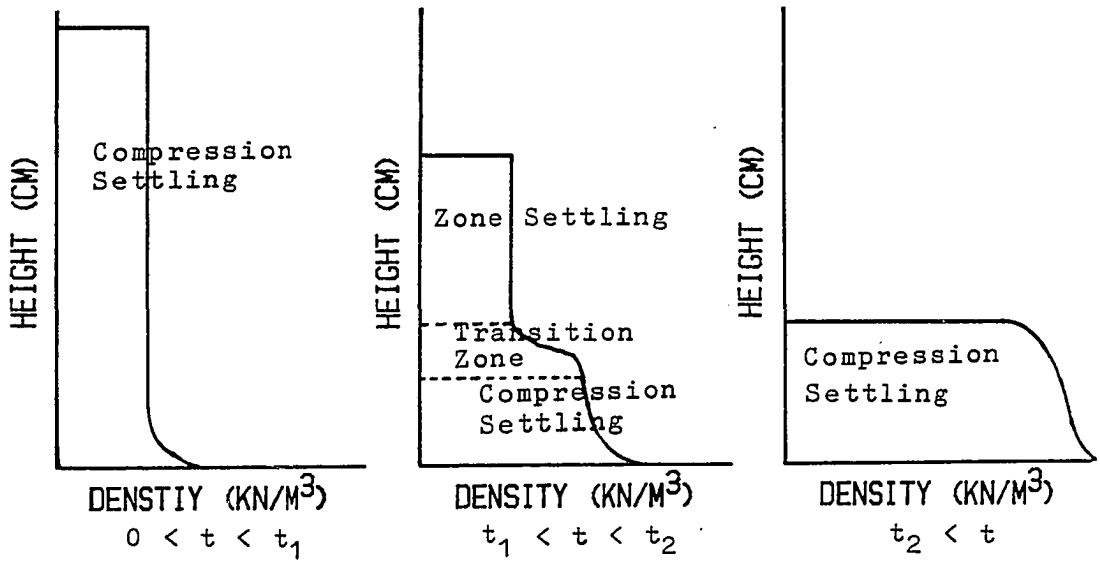

Figure 11. Schemaatic of density changes with height in time

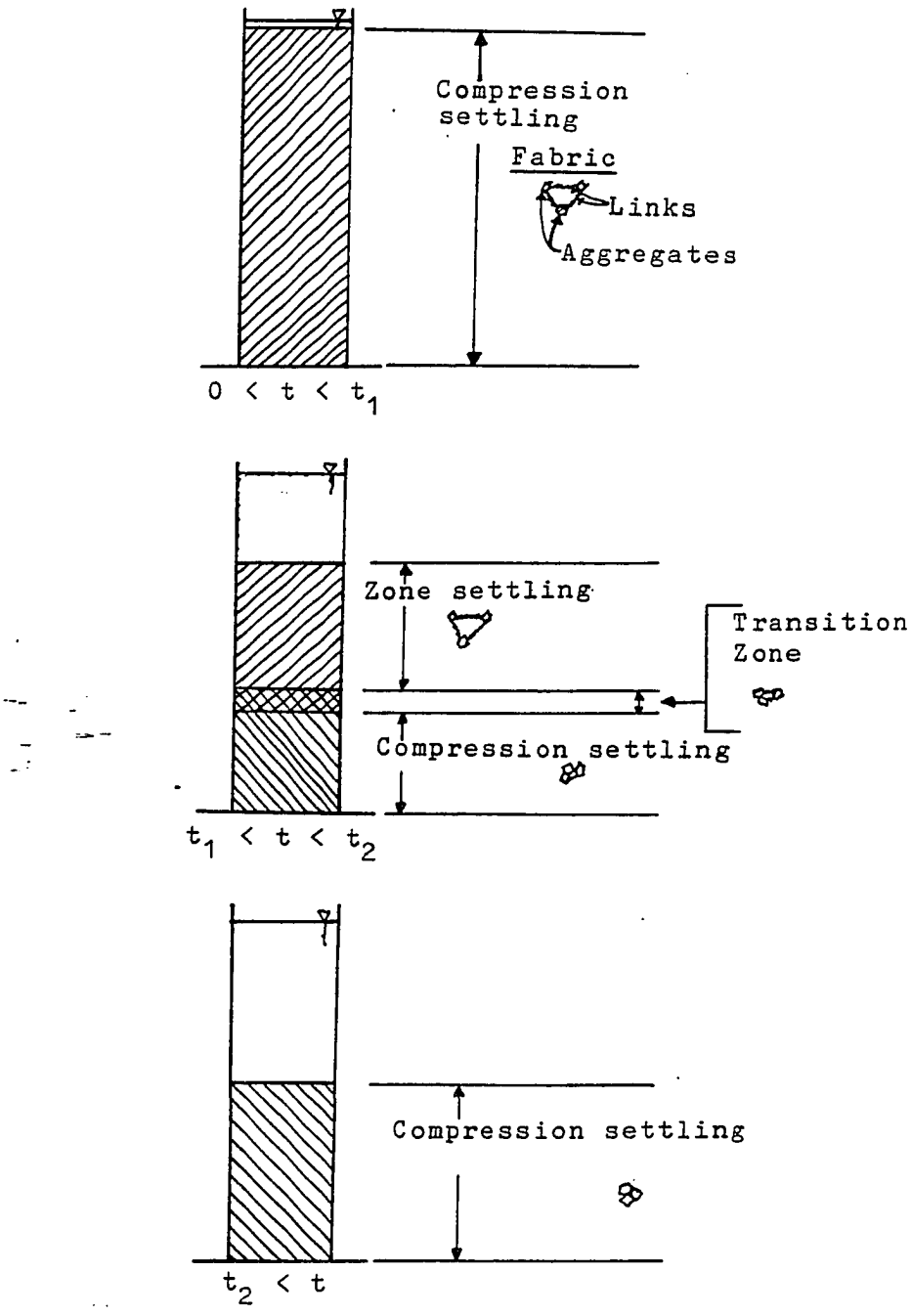

Figure 12. Schematic of structural changes with height in time

collapse has not occurred.

For $t_1 < t < t_2$, collapse has occurred. The fabric in the zone settling phase is equivalent to the fabric in the initial compression settling phase. In the transition zone, the links have broken in most cases and the aggregates are more closely arranged as they enter the compression settling phase. In the final compression settling phase, $t_2 < t$, the remaining links collapse and the aggregates themselves are being reformed. The compression process continues with time.

The large strain consolidation equation is again restated as follows:

$$\frac{\partial e}{\partial t} = -\frac{\partial}{\partial z}\left(\frac{K(e)}{\rho_f (1+e)}\frac{d\sigma'}{\partial e}\frac{\partial e}{\partial z}\right) - \left(\frac{\rho_s}{\rho_f} - 1\right)\frac{d}{de}\left(\frac{K(e)}{(1+e)}\right)\frac{\partial e}{\partial z} \qquad (2)$$

Been and Sills (1981) suggested that the relationship between permeability and void ratio to be linear as expressed in Equation (4). By assuming a linear relationship, the right hand term of Equation (2) becomes zero. It is suggested that such a relationship is unreasonable and that a relationship as described by Poiseuille's law may be more reasonable. Taylor (1948) used Poiseuille's law to derive a relationship between permeability and void ratio:

$$K(e) = D_s^2 \frac{\gamma_w e^3}{\mu(1+e)} C \qquad (10)$$

D_s is the average grain size, γ_w is the unit weight of water, μ is the viscosity, e is the void ratio, and C is a composite shape factor. These factors will be combined, with the exception of void ratio, to give the

following equation:

$$K(e) = C_p \frac{e^3}{1+e} \tag{11}$$

Where $C_p = D_s^2(\gamma_w/\mu)C$ which is a function of the grain size and fluid properties as well as the structure. C_p will have two different values for channeling and non-channeling. Recently, Samarasinghe et al. (1982) has suggested a slight alteration to this equation for permeability by substituting an n in for the 3 in Equation (11), where n varies depending on the soil or material of interest. Equation (11) will be used for the purposes of this study, but later studies should give consideration to other alternatives for the relationship of permeability and void ratio. The purpose here is to show that by assuming a more rationale relationship between permeability and void ratio, rather than the linear relationship assumed by Lee and Sills (1981) the advection portion of the large strain consolidation equation does not drop out but remains intact.

With substitution of Equation (11) into Equation (2), the large strain consolidation equation will take on the following form:

$$\frac{\partial e}{\partial t} = C_F \frac{\partial^2 e}{\partial z^2} - \left(\frac{\rho_s}{\rho_f} - 1\right) \frac{d}{de}\left(C_p \frac{e^3}{(1+e)^2}\right) \frac{\partial e}{\partial z} \tag{16}$$

C_F is assumed constant for an individual settling test.

The value of C_p will depend upon the mechanism of settlement. During compression, there is no channeling and therefore, permeability will be far less for equivalent void ratios. C_p for this region will

be labeled C_{p1}. In the region of zone settling, channeling occurs and C_p will be labeled C_{p2}. The equations for the regions will be expressed as follows:

Compression settling:

For $(0 < t < t_1)$, and $(t_1 < t$, and $e < e_a)$

$$\frac{\partial e}{\partial t} = C_F \frac{\partial^2 e}{\partial z^2} - \left[\left(\frac{\rho_s}{\rho_f} - 1 \right) C_{p1} \frac{e^2(3+e)}{(1+e)^3} \right] \frac{\partial e}{\partial z}$$

Zone settling:

For $(t_1 < t)$, and $e_a < e)$

$$\frac{\partial e}{\partial t} = C_F \frac{\partial^2 e}{\partial z^2} - \left[\left(\frac{\rho_s}{\rho_f} - 1 \right) C_{p2} \frac{e^2(3+e)}{(1+e)^3} \right] \frac{\partial e}{\partial z}$$

The void ratio e_a represents the boundary between zone and compression settling. In the compression zones, the advection terms influence is minimal because of the small values of permeability. That is why those modeling compression settling have been successful when ignoring this term.

CONCLUSIONS

The foregoing discussion suggests that the interface versus time curves from settling tests by Lin (1983) and Fuerstenau (1960) may be interpreted such that a metastable structure forms in the slurry. The theories used by mining, chemical, and sanitary engineers have used purely mathematical models or emphasized sedimentation phenomena in which the particles are born by hydrodynamic forces. Geotechnical engineers have emphasized the consolidation aspects of the settling process, but in all disciplines the transition from one mechanism to another has been poorly defined. The large strain consolidation theory of Gibson et al. (1967) may be used to model this phenomenon and help to more clearly define this transition.

REFERENCES CITED

Been, K. 1980. Stress Strain Behaviour of a Cohesive Soil Deposited Under Water. Ph.D Dissertation. University of Oxford, United Kingdom.

Been, K. and G. C. Sills. 1981. Self-Weight Consolidation of Soft Soils: An Experimental and Theoretical Study. Geotechnique 31(4):519-535.

Coe, H. S. and G. H. Clevenger. 1916. Methods for Determining the Capacities of Slime-Settling Tanks. American Institute of Mining Engineers Transactions 55(9):356-384.

Dell, C. C. and M. B. Kaynar. 1968. Channeling in Flocculated Suspensions. Filtration and Separation 5:323-327.

Dick, R. I. and B. B. Ewing. 1967. Evaluation of Activated Sludge Thickening Theories. American Society of Civil Engineers 93(SA4):9-29.

Fitch, B. 1962. Sedimentation Process Fundamentals. American Institute of Mining Engineers Transactions 223:129-137.

Fuerstenau, M. C. 1960. The Mechanism of Thickening Kaolin Suspensions. Ph.D. Dissertation. Massachusetts Institute of Technology, Cambridge, Mass.

Gaudin, A. M. and M. C. Fuerstenau. 1962. Experimental and Mathematical Model of Thickening. American Institute of Mining Engineers Transactions 223:122-129.

Gaudin, A. M., M. C. Fuerstenau, and S. R. Mitchell. 1959. Effect of Pulp Depth and Initial Pulp Density in Batch Thickening. American Institute of Mining Engineers Transactions 214:613-616.

Gibson, R. E., G. L. England, and M. J. L. Hussey. 1967. The Theory One-Dimensional Consolidation of Saturated Clays. Geotechnique 17(3):261-273.

Kynch, C. J. 1952. A Theory of Sedimentation. Faraday Society Transactions 48:166-176.

Lawler, D. F., P. C. Singer, and C. R. O'Melia. 1982. Particle Behavior in Gravity Thickening. Journal of Water Pollution Control Federation 54(10):1388-1400.

Lee, K. and G. C. Sills. 1981. The Consolidation of a Soil Stratum, Including Self-Weight Effects and Large Strains. International Journal for Numerical and Analytical Methods in Geomechanics 5:405-428.

Lin, T. W. 1983. Sedimentation and Self Weight Consolidation of Dredge Spoil. Ph.D. Dissertation. Iowa State University, Ames, Iowa.

Lin, T. W. and R. A. Lohnes. 1984. Sedimentation and Self Weight Consolidation of Dredge Spoil. ASCE Special Publication on Sedimentation/Consolidation Models, pp. 464-480.

Michaels, A. S. and J. C. Bolger. 1962. Settling Rates and Sediment Volumes of Flocculated Kaolin Suspensions. Industrial and Engineering Chemistry Fundamentals 1:24-33.

Mitchell, J. K. 1976. Fundamentals of Soil Behavior. John Wiley and Sons, Inc., New York, NY.

Pusch, R. 1970. Microstructural Changes in Soft Quick Clay at Failure. Canadian Geotechnical Journal, 7(1):1-7.

Samarasinghe, M. A., Y. H. Huang, and V. P. Drnevich. 1982. Permeability and Consolidation of Normally Consolidated Soils. American Society of Civil Engineers, 108(GT6):835-850.

Schiffman, R. L., V. Pane, and R. E. Gibson. 1984. The Theory of One-Dimensional Consolidation of Saturated Clays. ASCE Special Publication on Sedimentation/Consolidation Models:1-29.

Taylor, D. W. 1948. Fundamentals of Soil Mechanics. John Wiley and Sons, Inc., New York, NY.

Vesilind, P. E. 1979. Treatment and Disposal of Wastewater Sludges. Ann Arbor Science Publishers, Inc., Ann Arbor, Mich.

Whitham, G. B. 1974. Linear and Nonlinear Waves. John Wiley and Sons, Inc., New York, NY.

Yong, R. N. and D. S. Elmonayeri. 1984. Convection-Diffusion Analysis of Sedimentation in Initially Dilute Solids-Suspensions. ASCE Special Publication on Sedimentation/Consolidation Models, pp. 260-274.

PART II. HYPOTHESIS OF SETTLING PHENOMENON: NUMERICAL EVIDENCE

INTRODUCTION

It was suggested in the theory and model proposal that flocculent suspensions form a continuous structure. This structure was defined as a metastable structure in which collapse occurs. This type of phenomenon has been suggested to be the cause of the reverse "S" shaped settling curves that have been observed. The large strain consolidation equation (Gibson et al., 1967) was suggested as the physical basis for modeling the settling process. The large strain consolidation equation has the form of an advection-diffusion equation which therefore lends itself to utilizing numerical techniques for solution which have already been developed in other fields such as groundwater contaminant transport.

REVIEW OF MODEL AND SIMPLIFICATIONS

Review

The proposed model is based on the large strain consolidation theory. The settling of a reverse "S" shaped settling test was partitioned into three zones (see Figure 1). Note that in an ideal settling test there would be two phases, eliminating the first compression zone. The advection-diffusion model was presented for these three zones and is restated as follows:

Compression settling:

For $(0 < t < t_1)$, and $(t_1 < t$, and $e < e_a)$

$$\frac{\partial e}{\partial t} = C_F \frac{\partial^2 e}{\partial z^2} - \left[\left(\frac{\rho_s}{\rho_f} - 1 \right) C_{p1} \frac{e^2(3+e)}{(1+e)^3} \right] \frac{\partial e}{\partial z}$$

Zone settling:

For $(t_1 < t$, and $e_a < e)$

$e_a < e$

$$\frac{\partial e}{\partial t} = C_F \frac{\partial^2 e}{\partial z^2} - \left[\left(\frac{\rho_s}{\rho_f} - 1 \right) C_{p2} \frac{e^2(3+e)}{(1+e)^3} \right] \frac{\partial e}{\partial z}$$

Simplifications

In the compression zones, the advection term's influence is minimal because of the comparatively small values of permeability. Been and Sills' (1981) model of compression settling has shown reasonable results

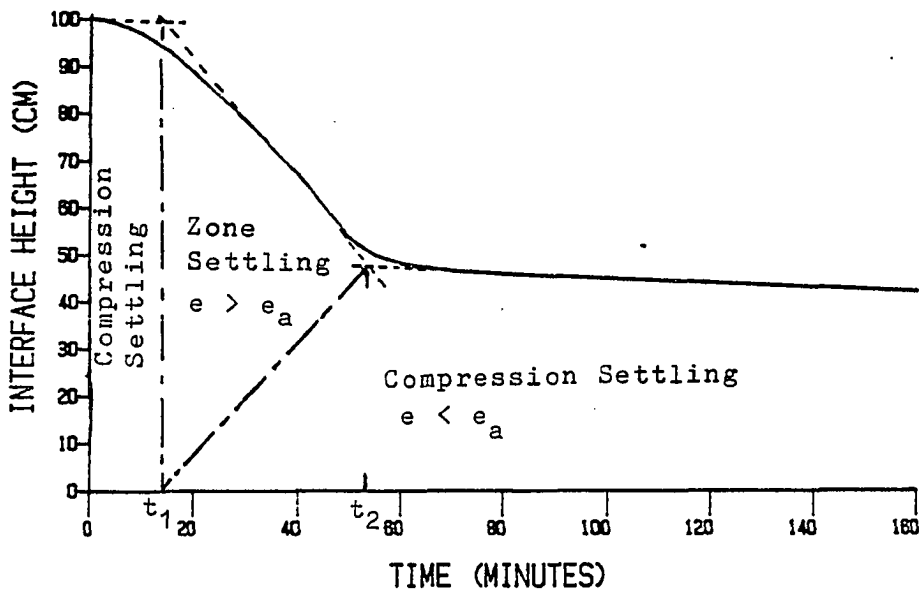

Figure 1. Reverse "S" shaped settling curve

for the compression settling phase. Their model is based solely on the diffusion term of the large strain consolidation equation. Therefore, the equation in the compression phases of the settling model is simplified as follows:

Compression settling:

For $(0 < t < t_1)$, and $(t_1 < t$, and $e < e_a)$

$$\frac{\partial e}{\partial t} = C_F \frac{\partial^2 e}{\partial z^2}$$

Zone settling:

For $(t_1 < t,\ e_a < e)$

$$\frac{\partial e}{\partial t} = C_F \frac{\partial^2 e}{\partial_z 2} - \left[\left(\frac{\rho_s}{\rho_f} - 1 \right) C_{p2} \frac{e^2(3+e)}{(1+e)^3} \right] \frac{\partial e}{\partial z}$$

OBSERVATIONS USED FOR MODELING

The settling test results used for modeling were those of Fuerstenau's (1960). These settling test results were unique in that density changes with depth of slurry and time were given. Fuerstenau (1960) observed the settling process of kaolin slurries with the use of an x-ray transviewer.

The percent solids by weight used in these tests were 9.1%, 11.1%, and 14.3%. Each of these tests was run at a constant flocculent concentration of 0.25 gm per liter CaO. The percent solids by weight ranging from 9.1% to 14.3% results in an initial void ratio range of 25.97 to 15.58, respectively. A glass cylinder was used with an I.D. of 9.4 cm and a height of 122 cm. Depth of slurry was initially started at 100 cm. The size range of particles was 2-20 μm. The specific gravity, G, was 2.6.

Figure 2 shows the density changes below the interface with time for the 11.1% solids by weight settling test. This is taken from Fuerstenau's data (1960). In the early periods of settling, density values are given for 15 vertical positions in the slurry at intervals of 6.25% of solids which represent points above which given amounts of solids are present. The first data point given from top to bottom is at the point where 6.25% of the solids lie above it. Therefore, the interface location is not directly given in the data with the exception of the 9.1% solids by weight settling test. Even though it is not given, the interface location can be determined. It can be determined by taking the slope de/dz at the 6.25% point and determining the height

required above that point for 6.25% of the solids. This method of locating the interface height is compared to the given location for the 9.1% solids by weight settling curve data (see Figure 3). By using this method, the settling curves for the three settling tests were determined as shown in Figure 4.

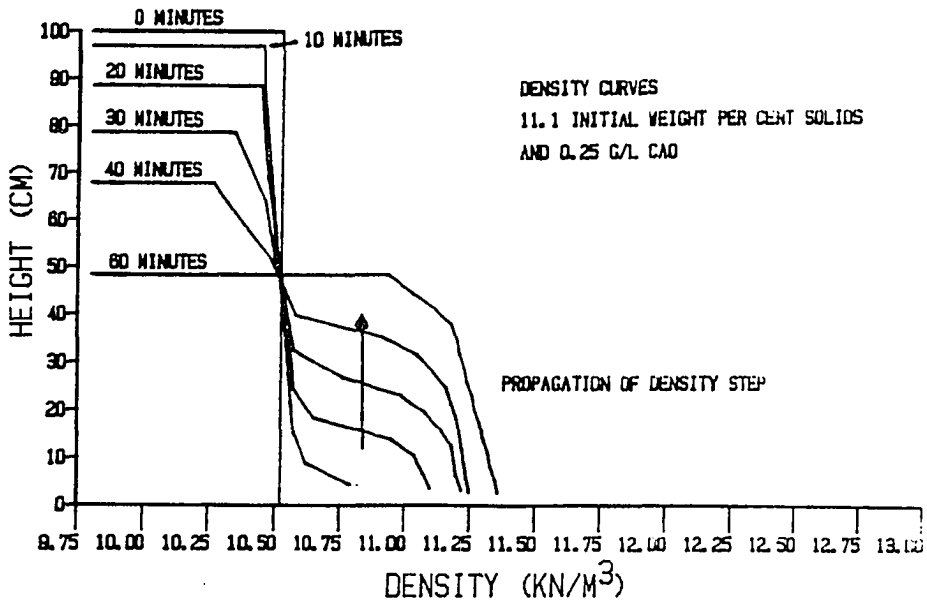

Figure 2. Density changes with depth and time (Fuerstenau, 1960)

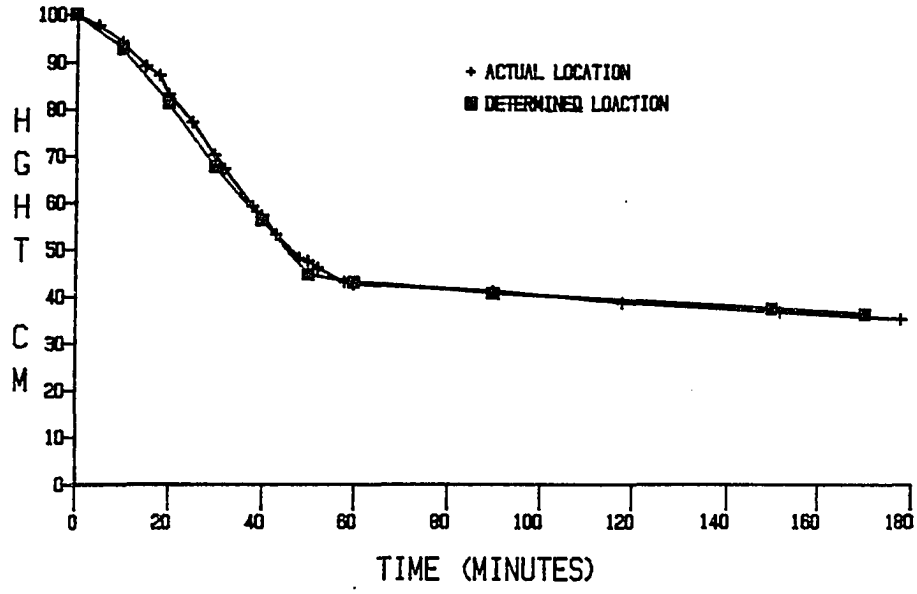

Figure 3. Comparison of actual and determined settling curves (Data are taken from Fuerstenau, 1960)

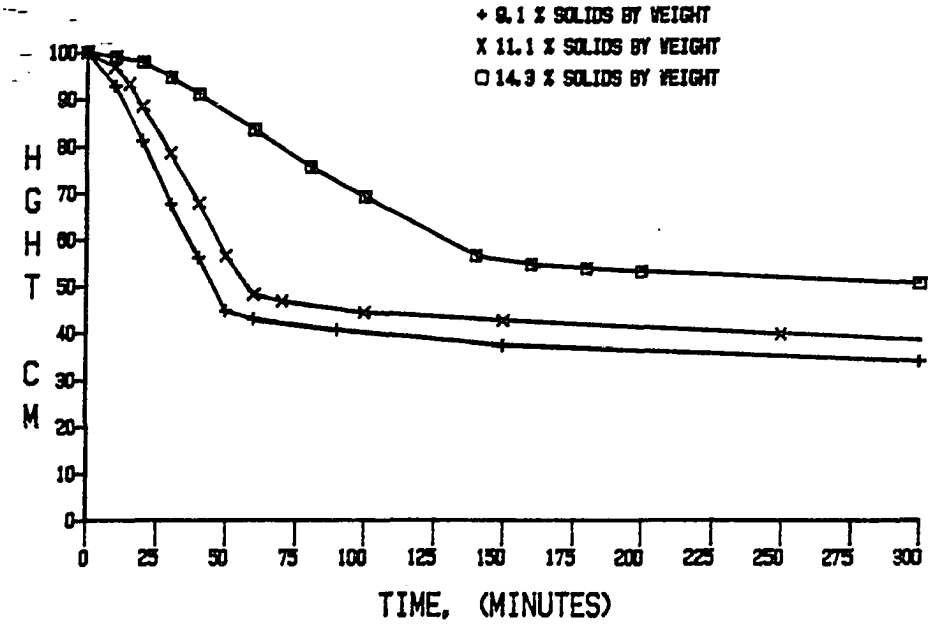

Figure 4. Settling curves for 9.1%, 11.1%, and 14.3% solids (Data are taken from Fuerstenau, 1960)

COMPUTER APPLICATION

Introduction

A finite element program was used to approximate the advection-diffusion equation that has been proposed. Recently, finite element techniques have been used to approximate the advection-diffusion equation in movement of groundwater contaminants. A finite element technique from this field of research (Wang and Anderson, 1982) has been adapted for approximating the large strain consolidation advection-diffusion equation. The adapted program is shown in Appendix A.

The large strain consolidation advection-diffusion equation is based on a material coordinate system rather than a spacial coordinate system. In the spacial coordinate system, the interface descends with time; whereas in the material system, the height of material remains constant. In the large strain consolidation equation, the void ratio moves through a fixed material coordinate system. Therefore, it is similar in nature to contaminant transport, where the change in contaminant concentration moves through a fixed spacial coordinate system.

Model Parameters

Advection

Advection has been proposed to be of primary importance in the region of zone settling. Figure 1 indicates this zone which begins at t_1 and ends at t_2. The equation for zone settling is as follows:

$$\frac{\partial e}{\partial t} = C_F \frac{\partial^2 e}{\partial z^2} - \left[\left(\frac{\rho_s}{\rho_f} - 1 \right) C_{p2} \frac{e^2(3+e)}{(1+e)^3} \right] \frac{\partial e}{\partial z}$$

The right hand term represents the advection term.

In Fuerstenau's data (1960), the minimum void ratio obtained for the period of testing was approximately 4.70. Figure 5 indicates that for void ratios greater than 4.0 the ratio of $e^2(3+e)/(1+e)^3$ is greater than 0.90 or roughly equivalent to one. It should also be noted that G = 2.6. Knowing these two relationships, the above equation becomes:

$$\frac{\partial e}{\partial t} = C_F \frac{\partial^2 e}{\partial z^2} - (1.6C_{p2})\frac{\partial e}{\partial z}$$

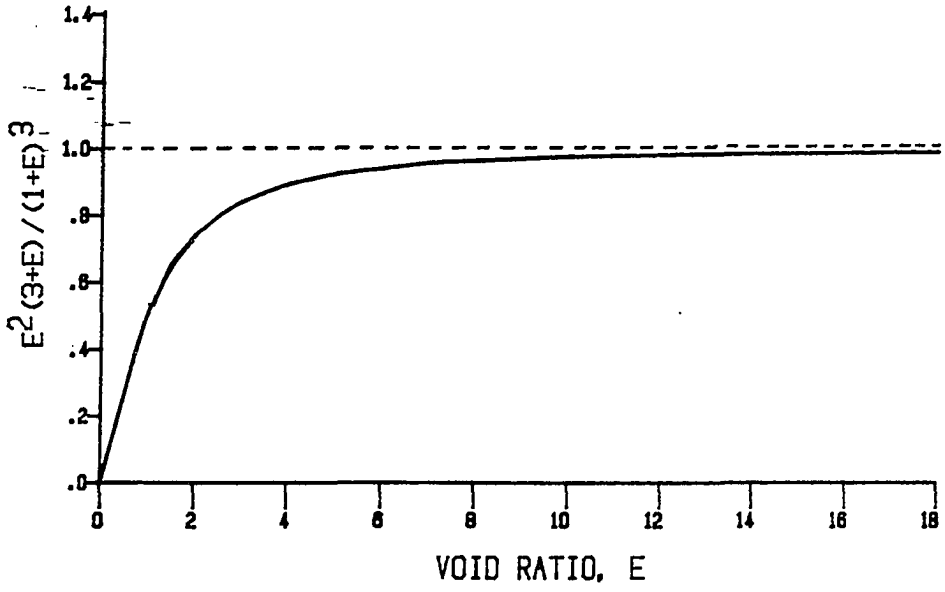

Figure 5. The relationship of $e^2(3+e)/(1+e)^3$ versus void ratio, e

In groundwater flow, the advection term represents the average

linear velocity of the contaminant front. It may be inferred from this that the advection term in the large strain consolidation equation represents the average linear velocity of the void ratio front. This velocity may be determined by estimating the time that it requires the initial density step to travel from the bottom of the slurry to the slurry/water interface. Time t_1 has already been designated as the beginning point and time t_2 as the point at which it reaches the surface. The average linear velocity, V_z, therefore is the total material height, z_t, divided by the elapsed time:

$$V_z = 1.6 \times C_{p2} = z_t/(t_2-t_1)$$

where:

V_z = average velocity of density step through the material coordinate system,

C_{p2} = constant,

z_t = total material height (cm)

t_1 = time at which density step begins (min)

t_2 = time at which density step reaches surface (min)

Table 1 shows the values for the three settling tests which were determined in this fashion. The table also shows the permeability value, k, which was determined from Equation (15) in Part I and e_i and C_p. The value e_a is the average void ratio of the slurry at t_2 and is used in the model as the void ratio at which diffusion becomes dominant and which advection becomes zero.

Table 1. Values for the three settling tests

Settling test no.	% by Wt. of solids	Initial void ratio, e	Material height z^a, cm	t_1 (min)	t_2 (min)	e_a	V_z cm/min	C_p cm/min	K cm/min
1	9.1	25.97	3.71	7.0	51	10.5	0.084	0.0527	34.22
2	11.1	20.82	4.58	11.0	55	9.28	0.104	0.0654	27.05
3	14.3	15.58	6.03	15.5	129	8.22	0.053	0.0335	7.64

[a] z is a material coordinate height and therefore remains constant through the settling process.

Diffusion

In the work carried out by Been and Sills (1981) on the self-weight consolidation of soft soils, an average diffusion value for settlement and density predictions was found to be suitable. Their experiments were carried out at various initial densities of the same material. It was therefore assumed that a single diffusion coefficient for the three settling tests being modeled would also be adequate. The C_F value was determined by a trial and error method. Settling test no. 1 was run with the predetermined parameters while changing the C_F parameter until the closest fit was obtained to the actual settling curve. The C_F parameter obtained was 0.025 cm^2/minute.

Boundary conditions

In modeling settling tests, there are two boundaries to be considered, the boundary at the bottom and the boundary at the slurry/water interface. The boundary at the bottom is considered impermeable and the void ratio of the material is continually decreasing with time. The flow condition therefore is in the upward vertical direction and is easily satisfied. The continually changing void ratio poses a problem but the data (Fuerstenau, 1960) for density change with time can supply the needed information for void ratio variation at the bottom boundary. Figure 6 shows the change in void ratio with time at the lower boundary of the three tests being modeled.

The upper boundary is also in a state of flux with time. The density will increase as the wave reaches the interface. It is also important to note that if the upper boundary is set at the slurry/water

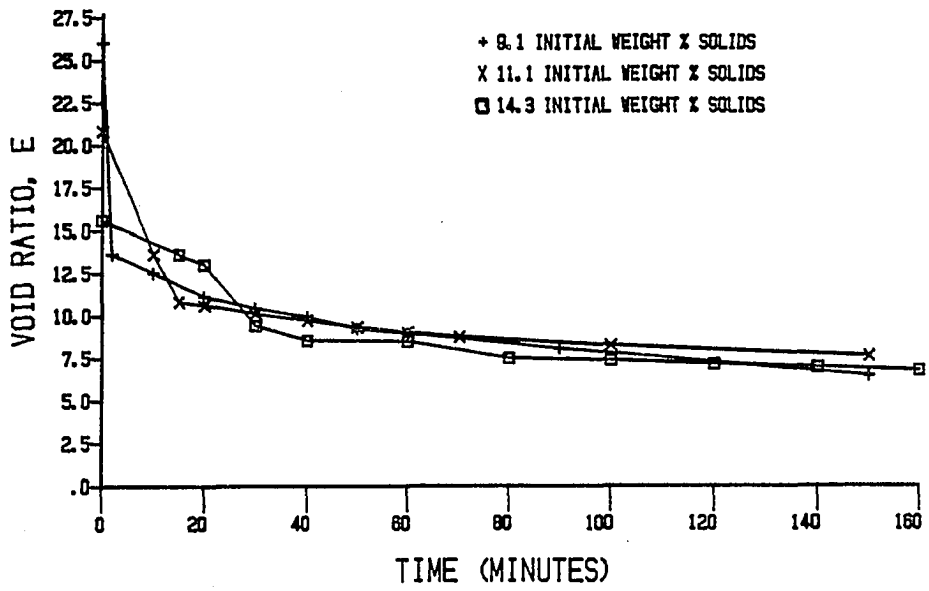

Figure 6. Void ratio change with time at lower boundary (Data are taken from Fuerstenau, 1960)

interface the finite element solution is limited to times less than the time needed for the density front to travel about two-thirds of the length z_t. If the latter requirement is not met, the solution will become unstable (see Figure 7). In order to allow the density step to reach the interface and also eliminate stability problems the upper boundary of the element mesh was extended beyond the slurry/water interface. Therefore, the density step could pass through the interface freely and stability problems were eliminated. A total of 17 elements and 36 nodes were used in modeling the three settling tests. Ten elements and 22 nodes were below the slurry/water interface. Figure 8

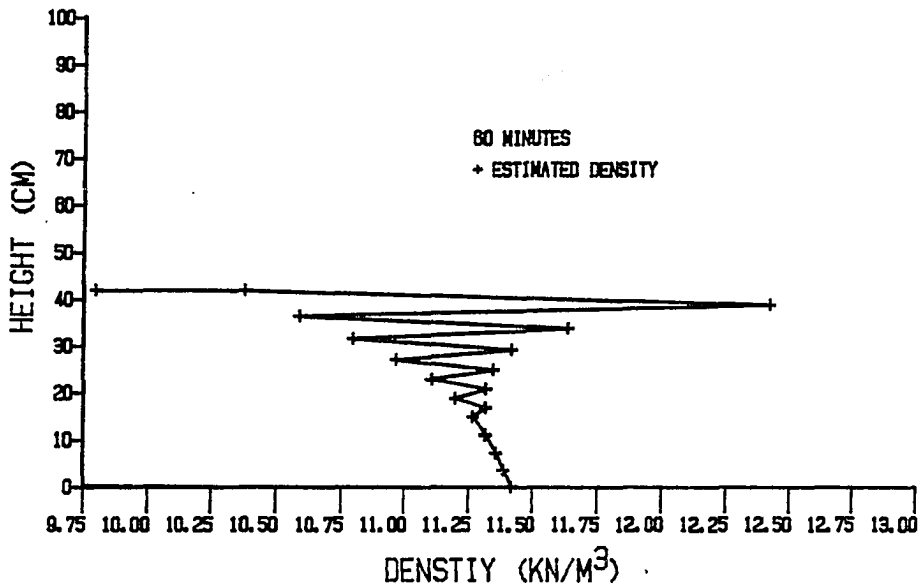

Figure 7. An unstable solution when wave front reaches upper boundary

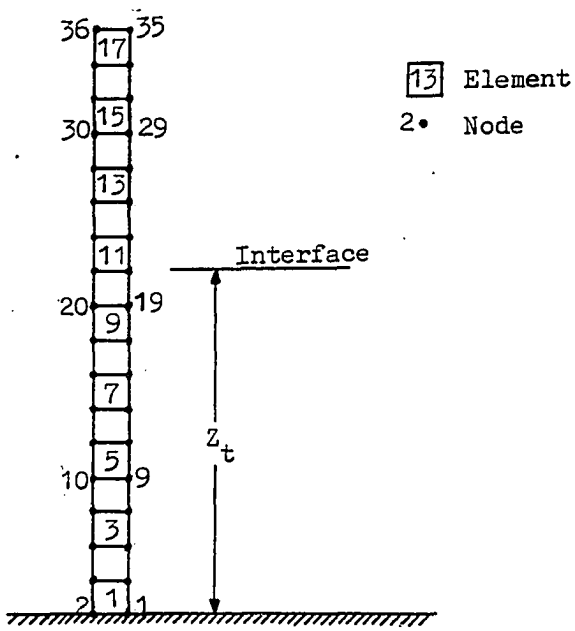

Figure 8. Element mesh and numbering system that was used

shows the element mesh and numbering system. The information supplied by the computer program was for the nodes at and below the slurry/water interface. The program carries on calculations in the material coordinate system and then converts answers to the spacial coordinate system in order to determine slurry/water interface descent.

DISCUSSION OF RESULTS

Settling Test Curves

Comparisons of the model and the actual settling tests were carried out for the first 160 minutes of each test. The actual and predicted interface settlement curves are shown in Figures 9, 10, and 11 for settling tests 1, 2, and 3, respectively. The settling curve results indicate that:

1. the assumption of an initial period of consolidation in reverse "S" shaped settling curves is reasonable;
2. the procedure for determining the advection term is reasonable; and
3. one diffusion term for the three tests resulted in reasonable predictions for each test.

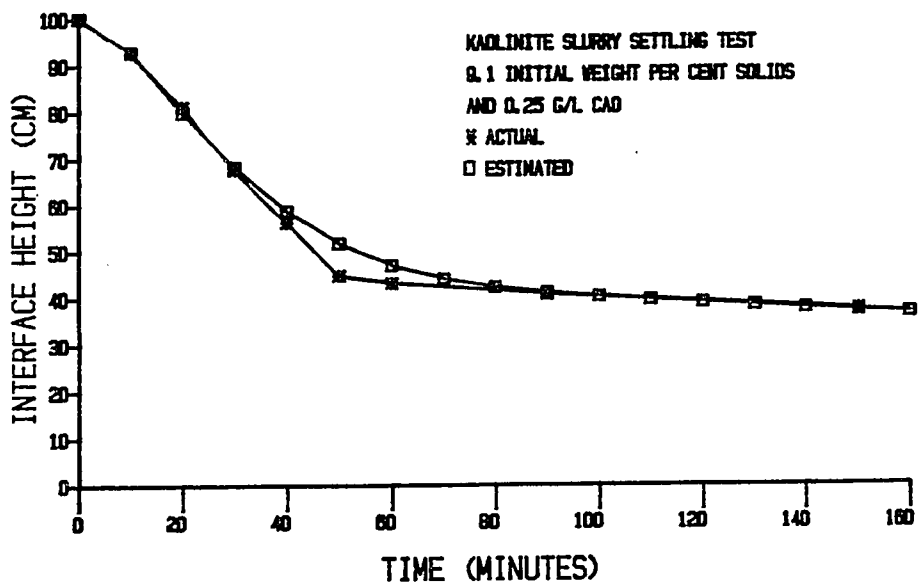

Figure 9. Results of modeling settling test no. 1

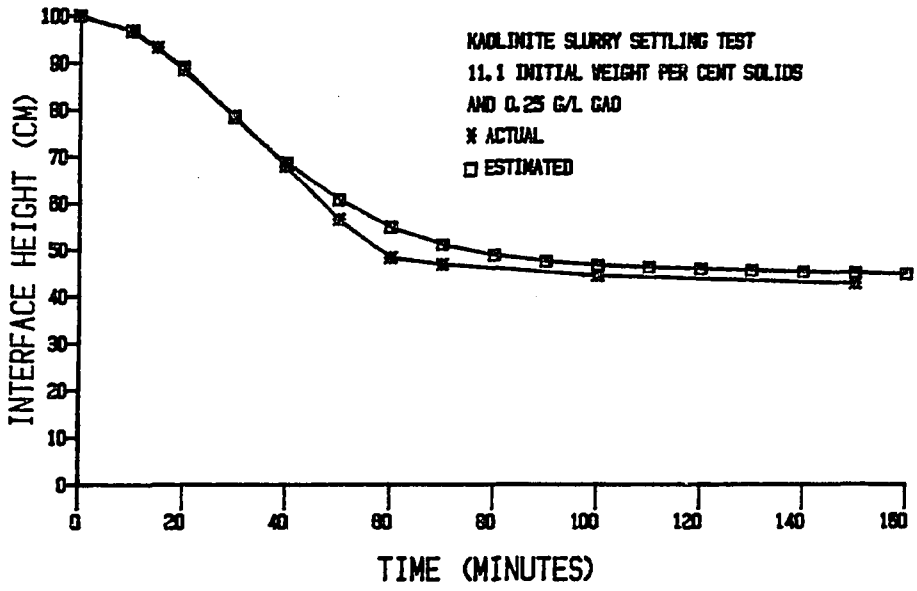

Figure 10. Results of modeling settling test no. 2

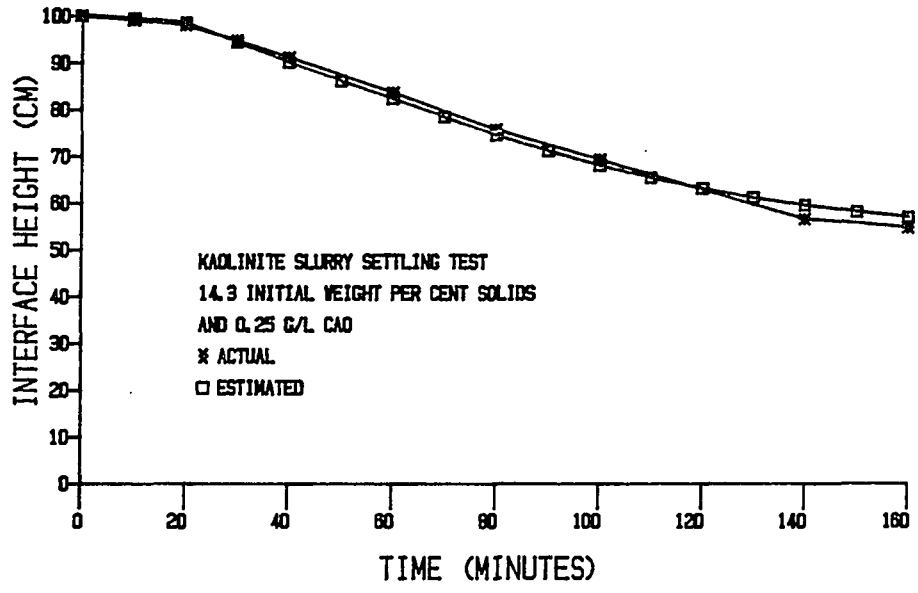

Figure 11. Results of modeling settling test no. 3

Density Curves

Estimated density curves and slurry height were determined at five minute intervals. A few of the curves for the 11.1 initial weight percent solids settling test are shown in Figures 12 through 18. The comparisons indicate:

1. the actual density near the upper boundary actually decreases initially before increasing. Whereas, the estimated densities steadily increased with time;
2. the density step is apparent in the actual case but appears to be strongly smoothed out in the estimated case; and
3. the later time periods show close agreement indicating that using the diffusion term without the advection term in the compression zone is reasonable.

The smoothing out of the density step in some degree plagues all numerical solutions of the advection-diffusion equation (Wang and Anderson, 1982). It is commonly called numerical dispersion and can be corrected by adding a correction term to erase some of the numerical dispersion. A correction term was not added in this case.

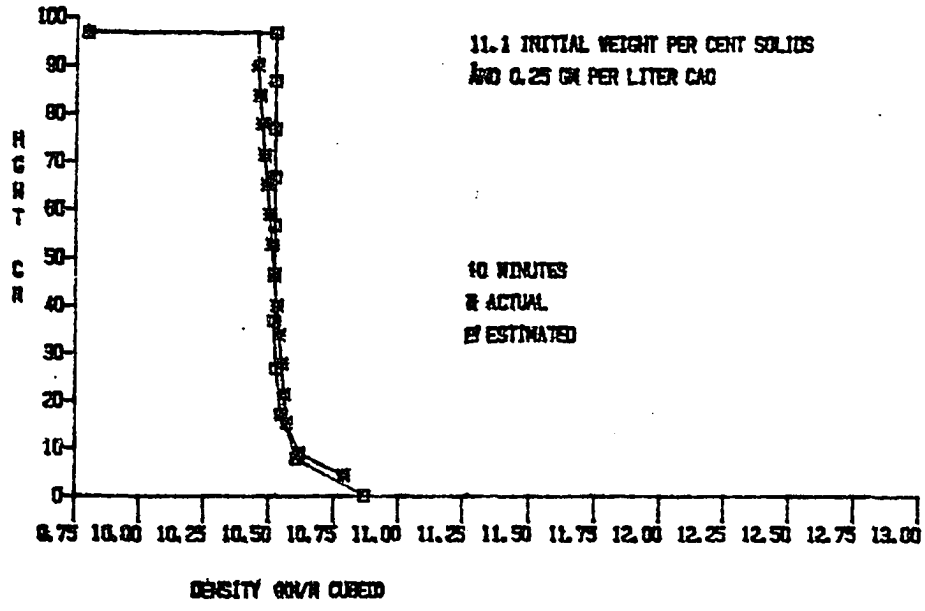

Figure 12. Results of modeling the density curve at 10 minutes for settling test no. 2

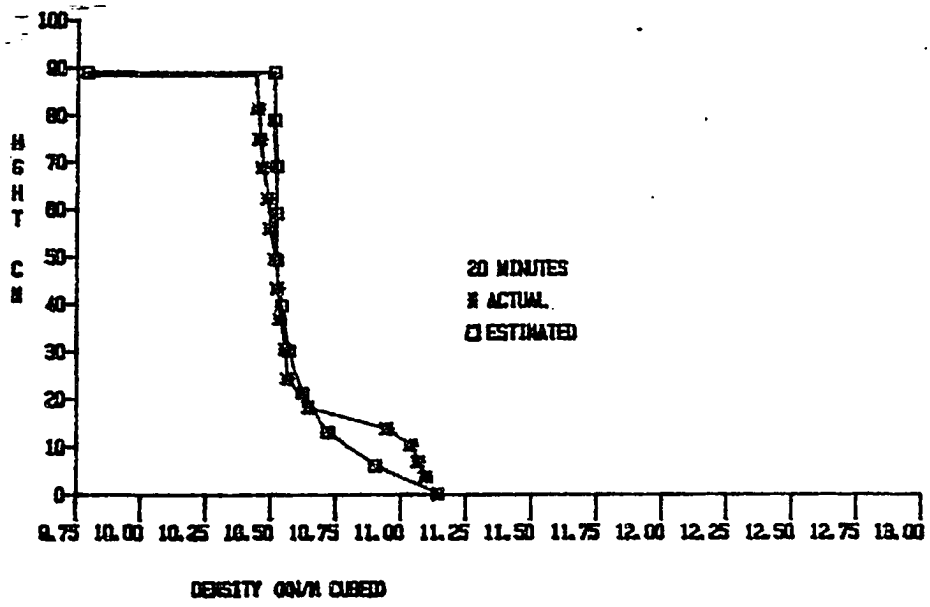

Figure 13. Results of modeling the density curve at 20 minutes for settling test no. 2

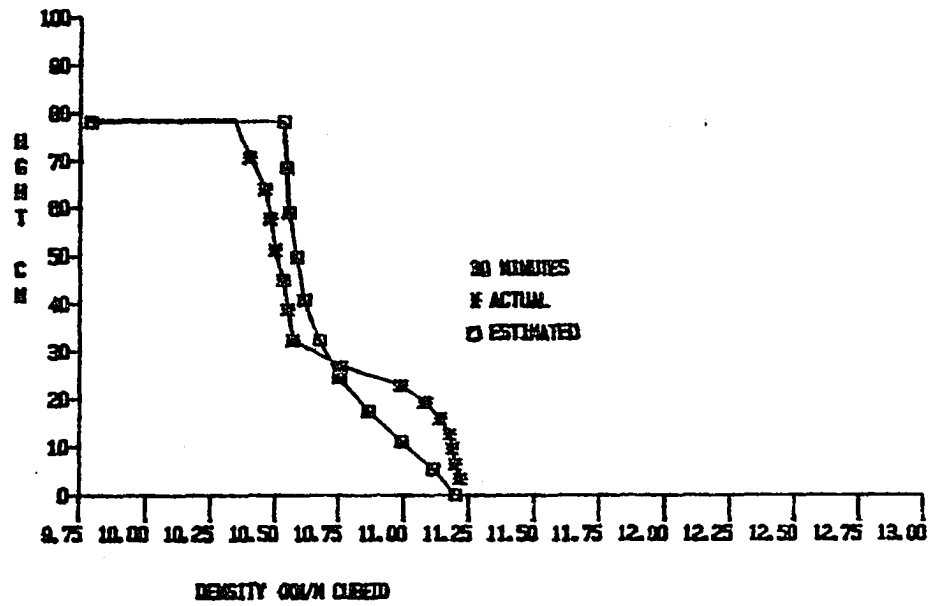

Figure 14. Results of modeling the density curve at 30 minutes for settling test no. 2

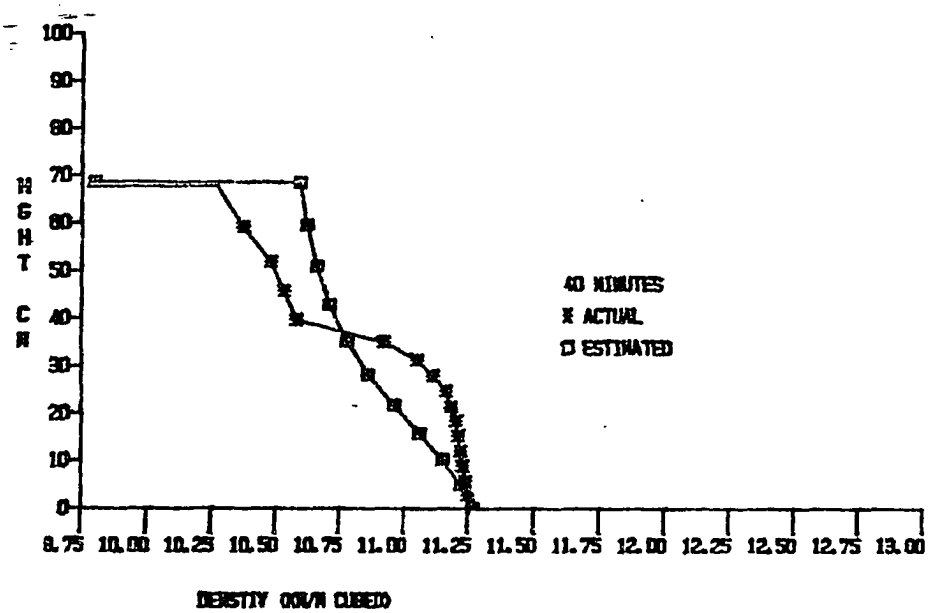

Figure 15. Results of modeling the density curve at 40 minutes for settling test no. 2

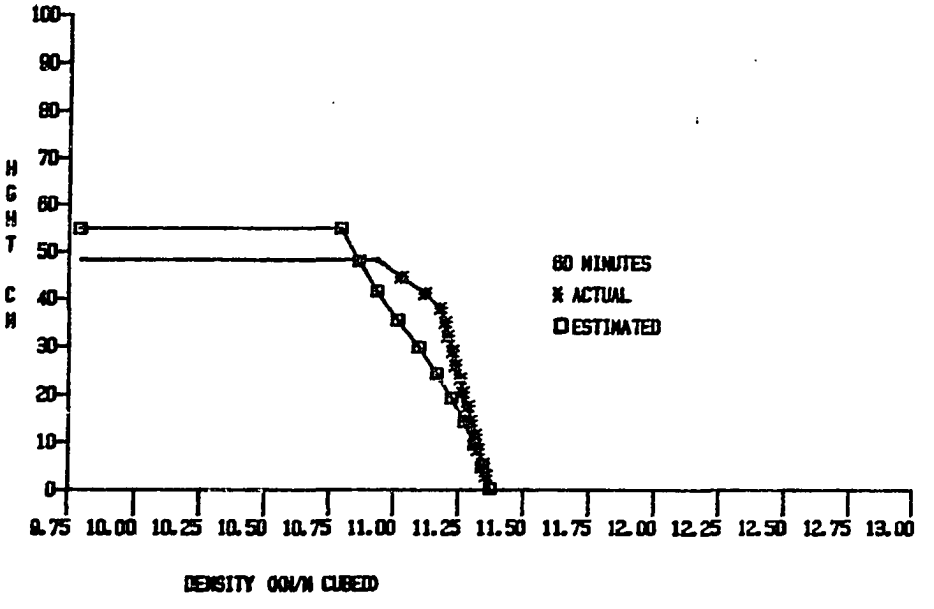

Figure 16. Results of modeling the density curve at 60 minutes for settling test no. 2

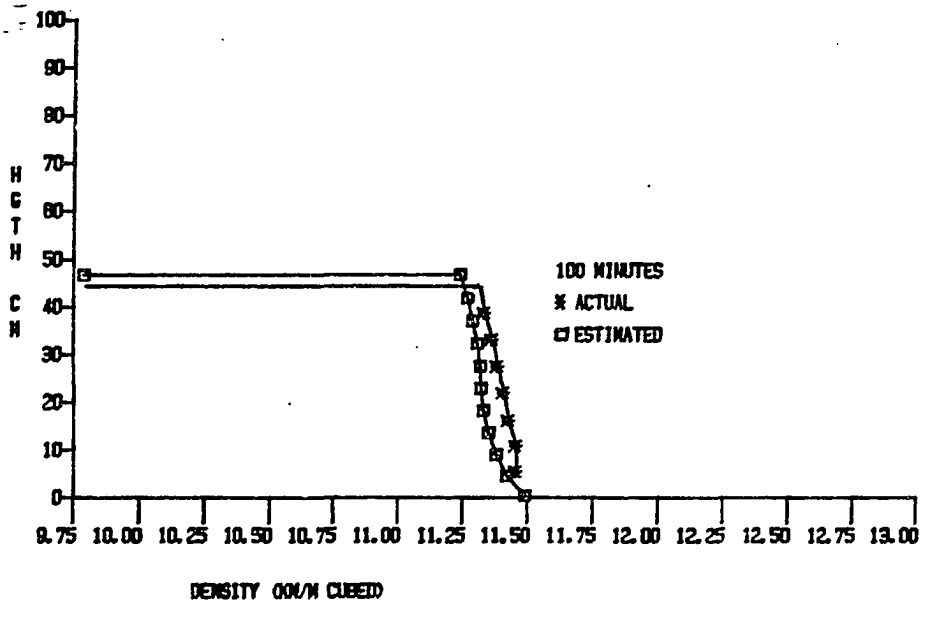

Figure 17. Results of modeling the density curve at 100 minutes for settling test no. 2

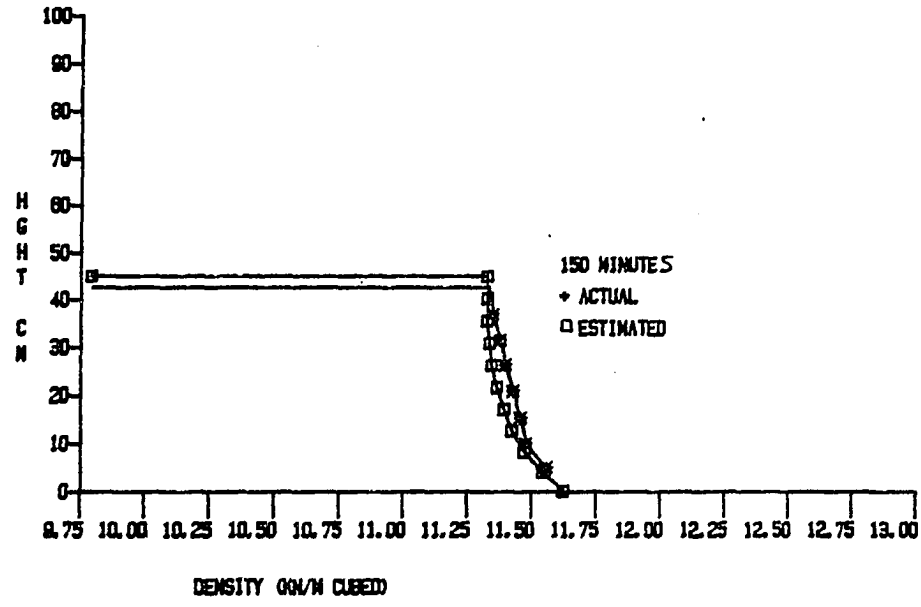

Figure 18. Results of modeling the density curve at 150 minutes for settling test no. 2

CONCLUSIONS

The large strain consolidation theory of Gibson et al. (1967) was formulated in terms of an advection-diffusion equation. The diffusion portion of the equation is dominant during the first phase of the process until the structure collapses. As the structure collapses, the advection term becomes an important factor, until the slurry enters the final compression phase of settling where diffusion once again dominates.

The model was tested numerically with a finite element solution and published data from Fuerstenau (1960) were used. The numerical evaluation of the new model gave good agreement with observations; however, the solution was possible because density variations at the bottom of the sedimentation column were known. These data were available because Fuerstenau (1960) used an x-ray transviewer to make his observations. A more economical instrument is needed to provide the necessary information to develop this model further.

REFERENCES CITED

Been, K. and G. C. Sills. 1981. Self-Weight Consolidation of Soft Soils: An experimental and Theoretical Study. Geotechnique 31(4):519-535.

Fuerstenau, M. C. 1960. The Mechanism of Thickening Kaolin Suspension. Ph.D. Dissertation. Massachusetts Institute of Technology, Cambridge, Mass.

Gibson, R. E., G. L. England, and M. J. L. Hussey. 1967. The Theory of One-Dimensional Consolidation of Saturated Clays. Geotechnique 17(3):261-273.

Wang, H. F. and M. P. Anderson. 1982. Introduction to Groundwater Modeling. W. H. Freeman and Company, San Francisco, California.

PART III. PREDICTING SETTLEMENT FOR EXTENDED PERIODS OF TIME

INTRODUCTION

An important factor in the design of dredge settling basins is the volume occupied by the dredge material after extended periods of time. This is important due to the costs of dike construction and earth work involved in preparing a containment area. A first approximation of the containment area volume required for storage of dredged material is often obtained by multiplying the in situ lake sediment volume by a bulking factor. Typical values of the bulking factor range from 1.0 for sands to 2.0 or greater for clays (Walsh and Bemben, 1981).

In order to make a more detailed approximation of the volume requirements, it is necessary to determine the long term changes in dredge material volume. This is of particular importance in cases where a containment area may be used year after year. There are some methods that have been used to estimate this change in volume with time. Three methods are reviewed and compared in this analyses: 1) a modified self weight consolidation model (Lin, 1983); 2) an exponential curve fitting method (Coulson and Richardson, 1955); and 3) a power curve fitting method (Montgomery, 1978). The settling tests used in this analysis are of natural sediment from Lake Panorama (Lin, 1983). Five settling tests from work carried out by Lin (1983) are shown in Figure 1. The concentrations of soil used in these tests varied from 75.3 g/l to 226.5 g/l. The methods are also compared to the sediment concentrations at the dredge containment site at the 55 day point. The containment area is located 5.2 miles upstream of the Lake Panorama dam in Guthrie County, Iowa.

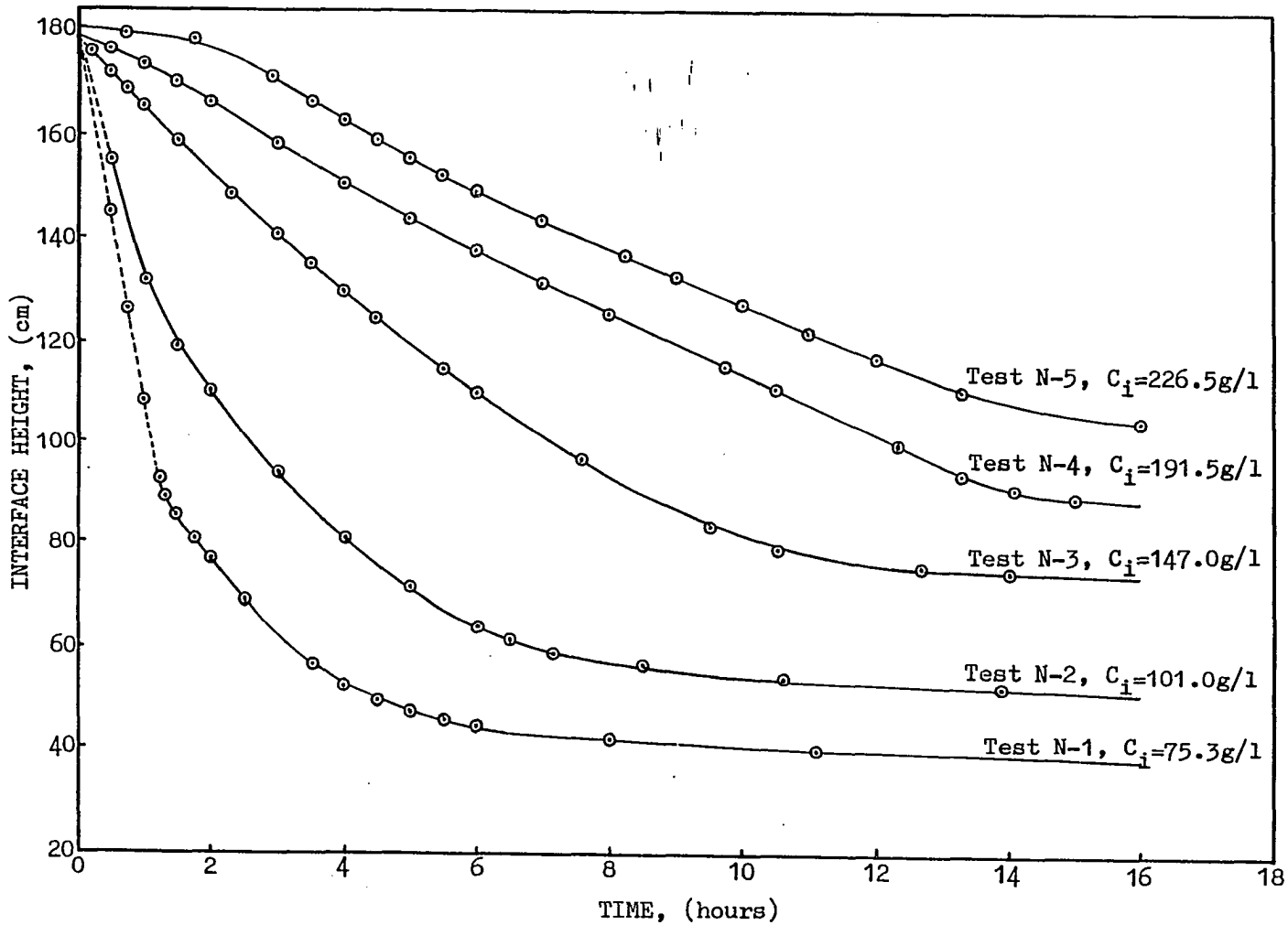

Figure 1. Lake Panorama sediment settling tests (Lin, 1983)

METHODS

Modified Self-Weight Consolidation Model

The rate of settlement for a specific material is characterized by a coefficient of consolidation. The model is based on the general equation governing large strain consolidation (Gibson et al., 1967) with the basic assumption that consolidation begins at the time of interface formation (Lin and Lohnes, 1984). Hence, the time and height and corresponding average concentrations at this time are referred to as critical values t_c, H_c, and C_c, respectively. The degree of consolidation $S_m(T')$, for the modified self-weight consolidation theory is expressed by the following equation:

$$S_m(T') = \frac{\sum_n \{[\frac{\sin Mr}{M^3} - \frac{r \cos Mr}{M^2}] \cdot [1 - \exp(-M^2 T)]\}}{\sum_n [\frac{\sin Mr}{M^3} - \frac{r \cos Mr}{M^2}]} \qquad (1)$$

and $T' = C_F t / z_0^2$

where:

T' = a dimensionless time factor,

t = time from t_c and not necessarily from the beginning of the settling test (days),

$M = m\pi = 1/2(2n + 1)\pi$; $\quad n=0,1,2,3,\ldots$

$r = z_1/z_0$ = a ratio of material heights,

C_F = coefficient of consolidation (cm^2/day), and

z_0 = a modified material height (cm).

A more complete explanation of these values and the theory is given by Lin and Lohnes (1984) and Lin (1983).

The equation for determining settlement after interface formation is as follows:

$$H(t) = H_c - (H_c - H_{100})S_m(T') \quad (2)$$

where:

H = material height at any time after t_c (days),

H_c = interface height at t_c(cm), and

H_{100} = the height of material after 100% primary consolidation (cm).

Table 1 is a summary of the values for the solution of Equations (1) and (2) (Lin, 1983). For test N-3, Equation (2) may therefore be expressed as follows:

$$H(t) = 176.8 - 129.0(S_m(T')) \quad . \quad (3)$$

The degree of consolidation, $S_m(T')$, is determined at each time step using Equation (1). The solution of $S_m(T')$ and $H(t)$ for test N-3 at various times is shown in Appendix B along with settling test data for the five tests shown in Figure 1.

Exponential Curve Fit Method

Coulson and Richardson (1955) assumed that the rate of consolidation of a slurry can be expressed by a first-order rate expression:

$$-dH/dt = i(H - H_\infty) \quad (4)$$

where:

Table 1. Summary of the conditions and results of settling tests (Lin and Lohnes, 1984)

Settling Test	Initial Conc. (g/l)	H_i (cm)	H_c (cm)	H_{100} (cm)	t_c (days)	z_0 (cm)	r	C_F cm^2/day
N-1	75.3	179.7	88.8	26.7	0.06	39.1	0.13	957
N-2	101.0	179.7	125.5	33.8	0.05	40.9	0.16	353
N-3	147.0	179.7	176.8	47.8	0.01	43.9	0.22	158
N-4	191.5	180.3	180.3	66.0	0.00	42.7	0.30	186
N-5	226.5	181.0	181.0	83.3	0.00	42.9	0.35	279

H = the height of interface at time t (cm),

H_∞= the ultimate height of the sediment (cm), and

i = constant for a given suspension.

The time for the interface to fall from H_c, the critical settling point, to a height H is expressed by the following:

$$-i(t-t_c) = \ln(H-H_\infty) - \ln(H_c-H_\infty) \qquad (5)$$

where:

t_c = time at which critical settling occurs (days),

H_c = interface height at critical settling point (cm).

The critical settling point is defined quite differently from that of Lin (1983). The critical settling point in this method represents the point at which the settling curve flattens out and enters what is frequently termed the compression settling phase.

$\ln(H-H_\infty)$ was plotted against $t-t_c$ for settling test N-3. A straight line fit was determined statistically resulting in a value for i. H_∞ was assumed equivalent to H_{100} of the previous method and H_c was 0.46 days. Figure 2 indicates the results and the following is an equation for determining H at a given time $(t-t_c)$ for settling test N-3:

$$H(t) = 28.18\ e^{-0.4379(t-t_c)} + 47.8 \qquad (6)$$

$$r^2 = 0.988;\ n = 7\ .$$

Power Curve Fit Method

Montgomery (1978) found that plots of average concentration versus time formed straight lines on log-log plots. He compared 15 day

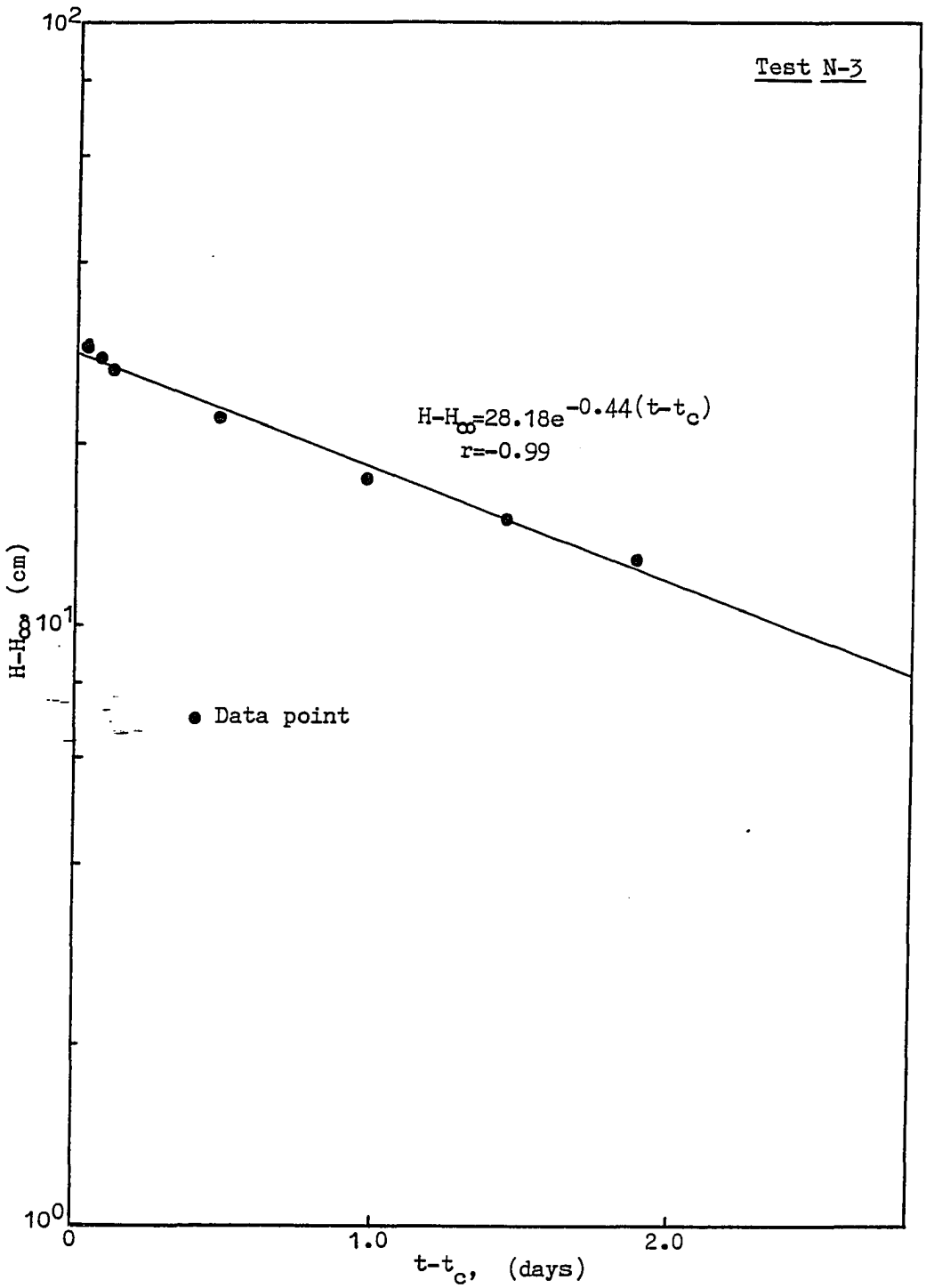

Figure 2. Determination of i for test N-3

settling tests with a 30x30 foot test basin. This method appeared reasonable and even though at some point in time consolidation will be complete and concentration will no longer continue to increase; the containment area storage requirements can be designed with confidence using this method (Montgomery, 1978).

The basic equation for determination of change in concentration with time is as follows:

$$C = at^b \tag{7}$$

where:

C = the average concentration (g/l),

t = time from the beginning of the settling test (days), and

a, b = constants for a given slurry.

The data for settling test N-3 were plotted on log-log as shown in Figure 3. The equation determined from these data is:

$$C = 383.7(t)^{0.15} \tag{8}$$

$$r^2 = 0.998; \quad n = 7 \quad .$$

The average concentration of a settling test is determined by the total dry weight of the soil divided by the total volume contained beneath the interface at that given time.

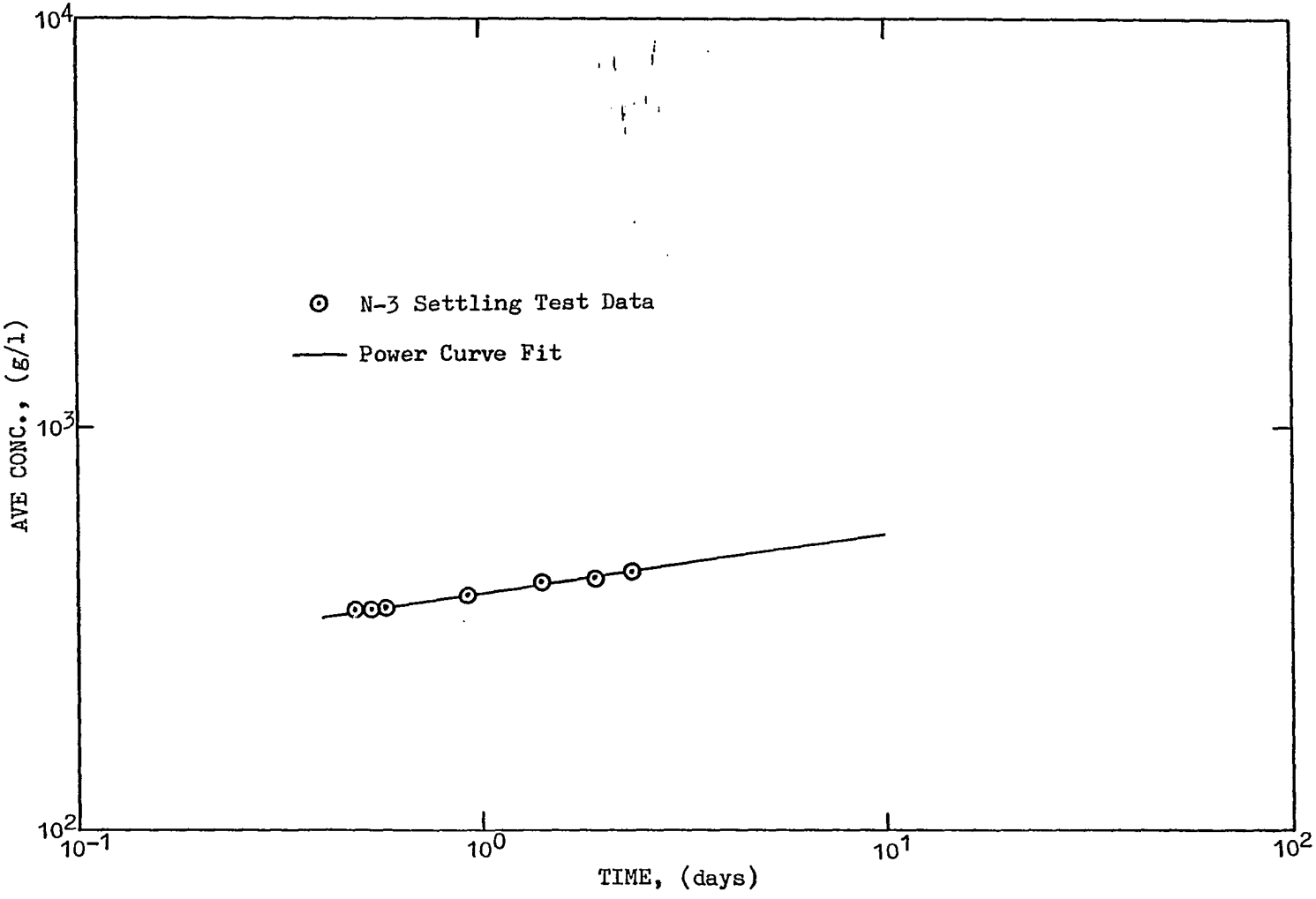

Figure 3. Power curve fit of compression settling data for test no 3

COMPARISON OF METHODS

The resulting equations for the three methods are compared in Figure 4. The H(t) values determined from the first two methods were converted to average concentrations and the three lines indicate the estimated values using these three equations. The settling data for test N-3 are also plotted along with seven concentration samples taken at 55 days at the Lake Panorama dredge material containment site (Vande Steeg, 1984).

It appears that the power curve fitting method passes through the cluster of samples at the fifty-five day point as well as the points it was fitted to. The exponential curve fitting method fits the settling test data well but falls below the field values. This is a reflection on the difficulty in determining the ultimate height, H_∞. With a proper selection of the ultimate density, this method would have passed through the field values as well. This points out one of the advantages of using the power curve fitting method in that a ultimate value is not required. Another advantage is that the power curve fitting method does not require long duration settling tests that are necessary for determining the ultimate height.

The modified self-weight consolidation method (Lin, 1983) is the only one of the three models compared in this analysis that attempts to estimate settling by physical modeling of the system rather than a purely empirical approach. The method does require settling tests for fitting purposes as is also required by the other two models. It is apparent that the method greatly underestimates the concentration values

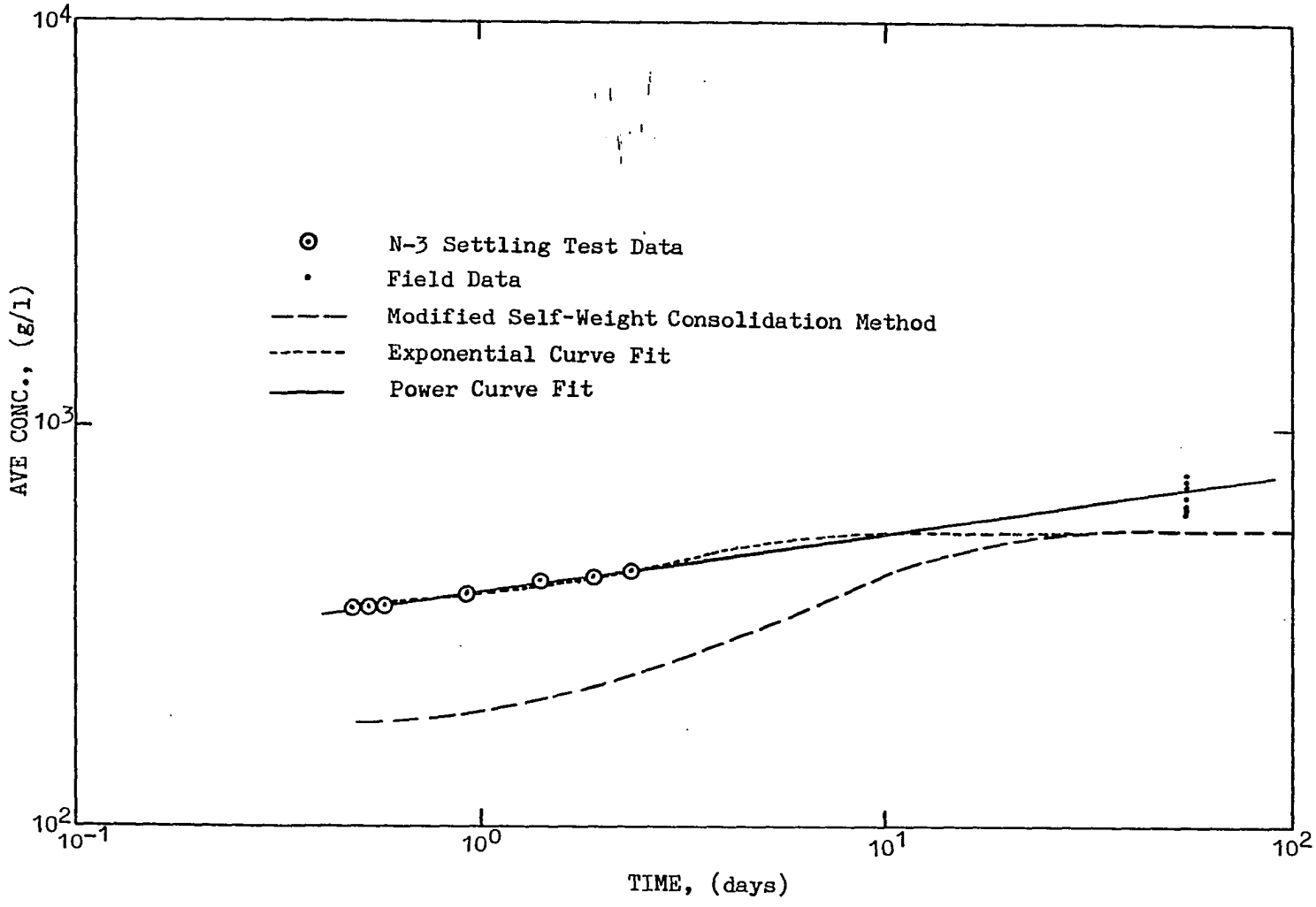

Figure 4. Comparison of methods on log-log plot

in the compression settling phase and is also hampered by the ultimate concentration requirement.

CONCLUSIONS

The power curve fitting method suggested by Montgomery (1978) appears to be adequate for design purposes and is actually easier to apply than the other two methods presented. There is also an additional advantage to presenting compression phase settling data as concentration values. Figure 5 is a plot of the compression phase of settling for the five tests presented in Figure 1. It can be observed that by plotting the data in this form the compression phase of settling is somewhat normalized.

The requirement of the ultimate consolidation, H_∞ is a difficult value to obtain and introduces an additional area for error. The power curve fitting method eliminates this requirement, simplifying the procedure.

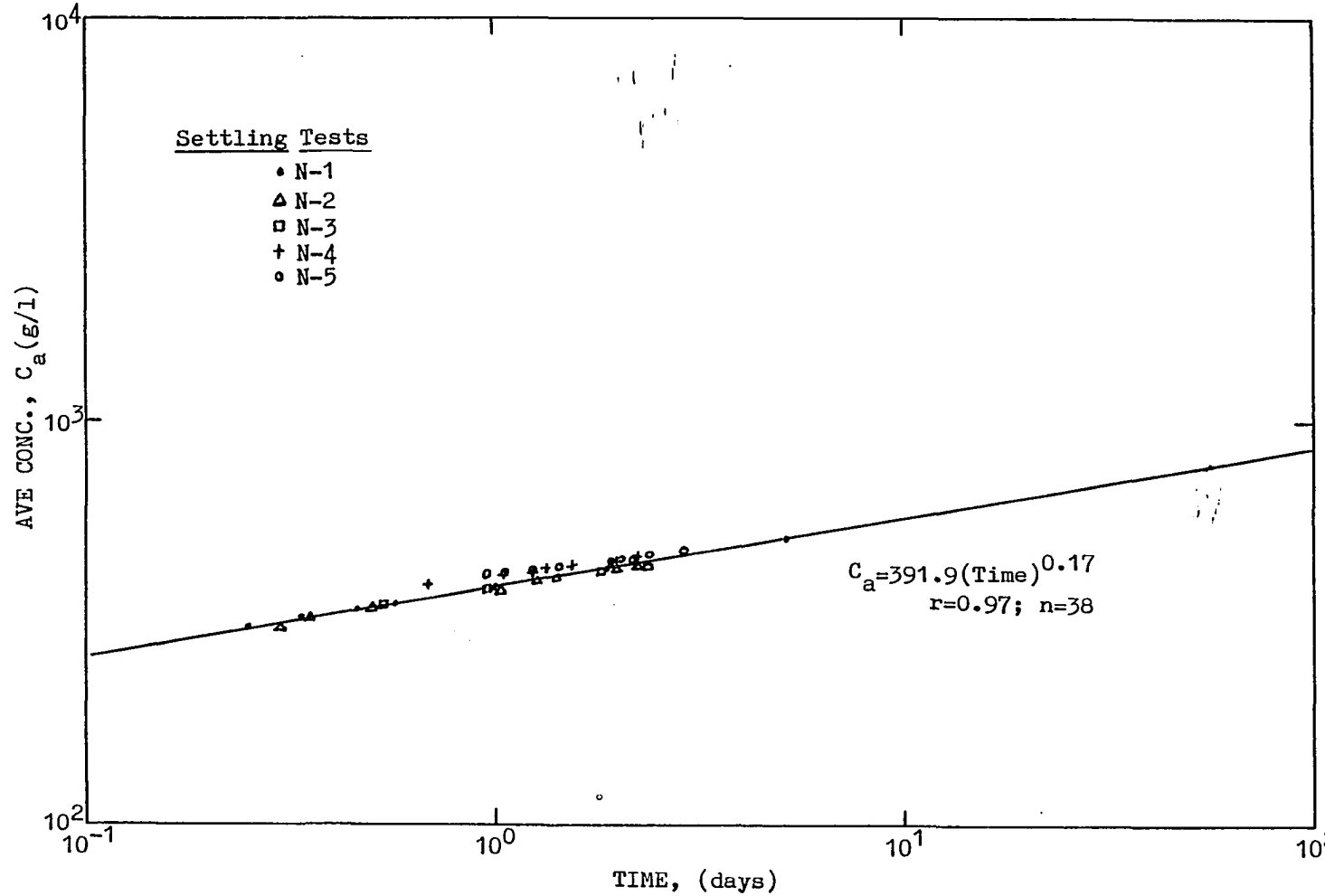

Figure 5. Average concentration values versus time for settling tests N-1, N-2, N-3, N-4, and N-5

REFERENCES CITED

Coulson, J. M. and J. F. Richardson. 1955. Chemical Engineering. Vol. 2. McGraw-Hill, Inc., New York, NY.

Gibson, R. E., G. L. England, and M. J. L. Hussey. 1967. The Theory of One-Dimensional Consolidation of Saturated Clays. Geotechnique 17(3):261-273.

Lin, T. W. 1983. Sedimentation and Self Weight Consolidation of Dredge Spoil. Ph.D. Dissertation. Iowa State University, Ames, Iowa.

Lin, T. W. and R. A. Lohnes. 1984. Sedimentation and Self-Weight Consolidation of Dredge Spoil. ASCE Special Publication on Sedimentation/Consolidation Models, pp. 464-480.

Montgomery, R. L. 1978. Methodology for Design of Fine-Grained Dredged Material Containment Areas for Solids Retention. U. S. Army Engineer Waterways Experiment Station, CE, Vicksburg, Miss., Technical Report D-78-56.

Vande Steeg, J. 1984. Professional Engineer, Shive-Hattery Engineers, Des Moines Iowa. Written Communication. March 21, 1984.

Walsh, J. E. and S. M. Bemben. 1981. Containment Area Design for Dredged Lake Materials. Proceedings of the ASCE Specialty Conference Water Forum, pp. 332-341.

PART IV. ELECTRICAL PROPERTIES OF SLURRIES

INTRODUCTION

In the last 25 years, there has been a great deal of research done on the thickening process of slurries (or sludges). These slurries have been studied by sanitary engineers for the thickening of particulates in wastewater treatment, mining engineers in the thickening of mineral tailings, and geotechnical and hydraulic engineers in the thickening of dredged materials. The thickening of slurries is dependent on the material being thickened and the medium in which it is settling. For this reason, the thickening process of slurries has to be studied on an individual basis. The typical instrumentation used in studying the thickening process of individual slurries is a sedimentation column in which observations of the slurry/water interface descent is recorded. Gaudin and Fuerstenau (1962) recognized that evaluation of the sedimentation process by observing the descent of the interface may be misleading. Therefore, Gaudin and Fuerstenau (1962) developed an x-ray transviewer to determine the change in density throughout the thickening process. Been (1980) used similar instrumentation for the same purposes.

X-ray transviewing is not commonly used for observing sediment thickening. The disadvantage to this technique is the cost of equipment. Another technique which has been used is to draw off samples at different levels in the sedimentation column. Lin (1983) discovered that drawing off samples disturbed the particulate matrix and altered the rate of settling, thereby accelerating the rate of settling. From this, it can be concluded that an instrument is needed for observing the

settling process with the following characteristics:

1. capable of determining density changes below the slurry/water interface at various times,
2. does not disturb the settling process,
3. economical enough for routine engineering design applications, and
4. is capable of determining the floc structure.

This section of the dissertation does not describe the development of such an instrument but rather, describes what is hoped to be necessary background research for the actual development of such an instrument. The dielectric constant and conductivity of high moisture content slurries were studied and results are shown here.

ELECTRICAL CONCEPTS AND DEFINITIONS

The capacitance C_0 for a parallel plate capacitor with its plates in a vacuum is defined by:

$$C_0 = q/V \tag{1}$$

where V is the potential difference applied across the plates and q is the charge that appears on the plates. The capacitance of a capacitor increases if a dielectric is placed between the plates. The ratio for the capacitance with the dielectric, C, to that without, C_0, is called the dielectric constant:

$$K = C/C_0 \quad . \tag{2}$$

The increased capacitance is due to polarization of the dielectric material. The molecules of some dielectrics, like water, have permanent electric dipole moments whereas, polarization is induced in other material by the electric field. As the dielectric material orients itself and becomes polarized in the electric field, this phenomenon gives the plates the ability to hold a greater charge.

For mineral components of most soils, the dielectric constant, K, is 2 to 4; whereas, for water it is approximately 80. This large difference between the dielectric constant of the solid and water phases in a slurry has led some researchers to conclude that the dielectric constant may be used as a measure of a mineral-water system's water content.

The most straightforward type of measurement for determining

dielectric constant values is to use direct current. This has been successful with electrically nonconducting sands and gravels. In a clay system however, direct current measurements cannot be used effectively because the electrokinetic effects may result in structural changes or reorientation of the solid phase; therefore, alternating current is used.

When alternating current is used, polarization plays an important role. The polarization may involve the following time-dependent processes:

1. Rapid processes: electronic, atomic, and ioinic polarizations. In this category, polarization is attained in less than 10^{-12} seconds.
2. Slow processes: resonance adsorption, interfacial, and orientation polarizations. In this category, polarization may take up to several minutes.

In the alternating current case, it is found that the measured responses are frequency dependent. When the polarization is not rapid enough to attain equilibrium with the alternating electric field, the current is 90° out of phase from the charging or capacitance component (Smyth, 1955).

The understanding of this phenomenon has led to the defining of a complex permittivity. Typically permittivity, ε, which is proportional to K is expressed by:

$$\varepsilon = K\varepsilon_0 \tag{3}$$

in which ε_0 = the permittivity of vacuum (equal to 8.85×10^{-12} f/mm in

the mks system of units). This expression includes only the effects of capacitance. The complex permittivity is defined from the concept of an effective complex capacitance which includes conductance:

$$\varepsilon^{*} = \varepsilon' - i\varepsilon'' \qquad (4)$$

$\varepsilon' = K\varepsilon_0$ and $\varepsilon'' = \sigma/\omega$

$i = \sqrt{-1}$

σ = conductivity (mhos/centimeter)

ω = angular frequency = $2\pi f$ where f is frequency (MHZ).

The angle δ between the total current vector and the charging current vector is called the loss angle. From this definition, it follows that:

$$\tan \delta = \frac{\varepsilon''}{\varepsilon'} = \frac{\sigma}{\omega K \varepsilon 0} \quad . \qquad (5)$$

Small values of tan δ correspond to a circuit which is primarily capacitive.

PREVIOUS RESEARCH

Most previous research investigations have measured soil capacitance, C, and resistance, R, with an impedance bridge. Capacitance and resistance are easily converted to dielectric constant, K, and conductivity, σ. These investigators have primarily been interested in the change in dielectric constant and conductivity with frequency (Arulanandan and Smith, 1973; Sachs and Spiegler, 1964; Smith and Arulanandan, 1981; Wobschall, 1977).

There have been other researchers who have investigated these properties for the purposes of determining moisture content (Thomas, 1966; Selig and Mansukhani, 1975; Lundien, 1971). Thomas (1966) correlated the change in capacitance to moisture density (rather than moisture content). Moisture density, M_v and moisture content, w are defined as follows:

M_v = weight of water/total volume (g/cc),

w = (weight of water/weight of solids) x 100.

Moisture density ranges from 0 to 1.00 g/cc, whereas moisture content ranges from 0 to infinity. Both moisture density and moisture content are used in this discussion where each is appropriate for presentation of the data. Typical soil moisture density studies have been in the range of 0 to 0.60; however, the moisture densities of slurries range from 0.80 to 1.00. In well logging, electrical measurements have been taken in formations which are 100% saturated but have moisture densities well below 0.80. Hence, the purpose of this study has been to determine

the applicability of dielectric constant and conductivity measurements in the soil moisture range of 0.80 to 1.00.

EXPERIMENT

The electrical measurements of slurries were performed using type 250 RX-meter (Booton Radio Corporation Division of Hewlett Packard, Rockway, NJ). The instrument is essentially a Scherring bridge, with oscillator, amplifier, detector, and null indicator, and is designed to measure equivalent parallel resistance, R_p, and capacitance, C_p. Resistance measurements range from 15 ohms to 100,000 ohms. Capacitance measurements range from 0 to 20 pico-farads. The frequency range is from 0.5 MHZ to 250 MHZ (1 MHZ = $1x10^6$ HZ). A similar instrument has been used by others to investigate soil-water systems (Arulanandan and Smith, 1981; Sachs and Spiegler, 1964).

The electrical measurements were conducted in the 5 MHZ to 90 MHZ range. Three types of soil slurries were tested; loess, Na-montmorillinite, and Lake Panorama sediment. The slurries were loaded into an electrical cell and connected to the RX-meter as shown in Figures 1 and 2. This cell is similar to the one used by Sachs and Spiegler (1964). One modification to the cell was required because with high moisture density slurries it was found that an air pocket became trapped in the cell which led to inconsistencies in results. A 0.80 mm diameter hole was drilled through the center of the upper plate in order to allow release of the trapped air.

This cell design and method of connecting it to the RX-meter was employed by Sachs and Spiegler (1964) to eliminate the impedance influences of the transmission line, the electrodes themselves, and the surroundings of the cell in general. The impedance effects were

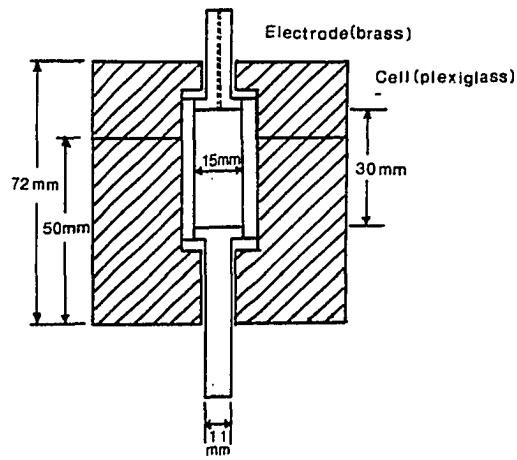

Figure 1. Cell for radio-frequency measurements at different electrode distances

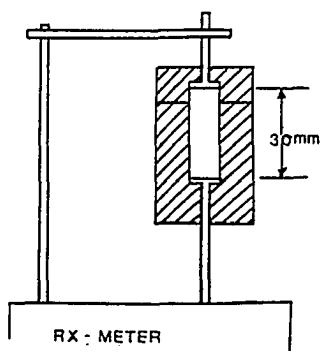

Figure 2. Representation of cell and transmission line connected to RX-meter

eliminated by measuring the electrical properties of the slurry at two different plate gaps. The true resistance, R_s, and capacitance, C_s, of the sample of greater length, at frequencies f is determined by the equations derived by Sachs and Spiegler:

$$R_s = \frac{\left[\frac{R_p^2(\Delta C)}{K} - \frac{R'^2_p(\Delta C')}{K}\right]^2 [K \cdot K']\ell\omega^2}{R_p K' - R'_p K](\ell-1)} + \frac{[R_p K' - R'_p K]\ell}{[K \cdot K;](\ell-1)} \qquad (6)$$

$$C_s = \left[\frac{(K \cdot K')(\ell-1)}{R_s\omega^2[R_p K' - R_p' K]\ell} - \frac{1}{R_s^2\omega^2}\right]^{1/2}$$

where

$$C = C_p - C_t$$

$$C' = C'_p - C_t$$

$$K = 1 + R_p^2\omega^2(C)^2$$

$$K' = 1 + R_p'^2\omega^2(C')^2$$

C_p and R_p = instrument readings at the greater length, ℓ

C_p' and R_p' = instrument readings at other length, and

C_t = the stray capacitance determined when cell is empty.

In this study, R_s and C_s were used in determining what is commonly called the apparent dielectric constant and the apparent conductivity. R_p and C_p were also used in evaluating what has been called the relative dielectric constant and relative conductivity. The values of R_p and C_p read directly from the instrument were converted to the relative dielectric constant and conductivity. The apparent values and relative values are compared to changes in moisture content which are discussed in the results.

RESULTS

Samples of loess, Na-montmorillinite, and Lake Panorama sediment were prepared with moisture densities ranging from 0.80 to 1.00 g/cc. Loess and Lake Panorama sediment were mixed with tap water. To improve the ease of preparation, Na-montmorillinite slurry samples were mixed with deionized water. Figures 3, 4, and 5 are plots of the R_p and C_p readings from 5 to 90 MHZ for loess, Na-montmorillinite, and Lake Panorama sediment, respectively. These plots are of data with the capacitor plate gaps set at 30 mm. A plate gap of 15 mm was also used for loess and Na-montmorillinite samples. It can be observed from Figures 3, 4, and 5 that R_p decreases with increased frequency and with decreased moisture density. C_p remains nearly constant but tends to increase slightly with increased frequency and increased moisture density.

Figure 6 shows the variation of the apparent dielectric constant, apparent conductivity and the loss factor, tan δ, versus moisture density for loess. The values at two frequencies of 5 MHZ and 90 MHZ are plotted. The apparent dielectric constant at 5 MHZ shows very little correlation to moisture density whereas the correlation at 90 MHZ is considerably better. The apparent conductivity shows very good correlation at both frequencies. This indicates that the apparent conductivity is a possible measurement for determining changes in moisture density; whereas, the apparent dielectric constant is a possible measuring technique at higher frequencies only. The disadvantage to using the apparent values is the complexity of the

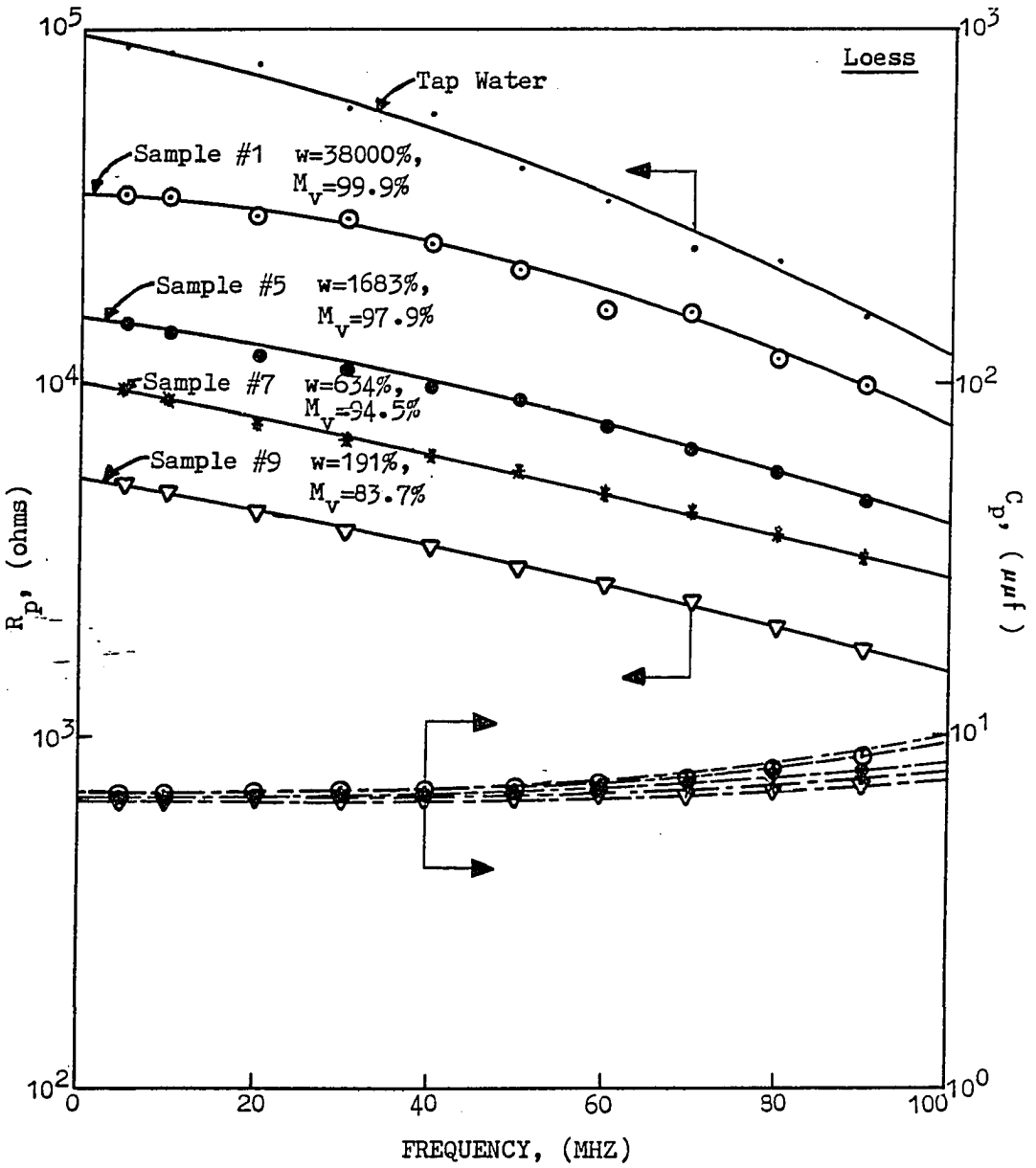

Figure 3. Rx-meter 250-A readings for loess samples; parallel resistance (R_p) and parallel capacitance (C_p)

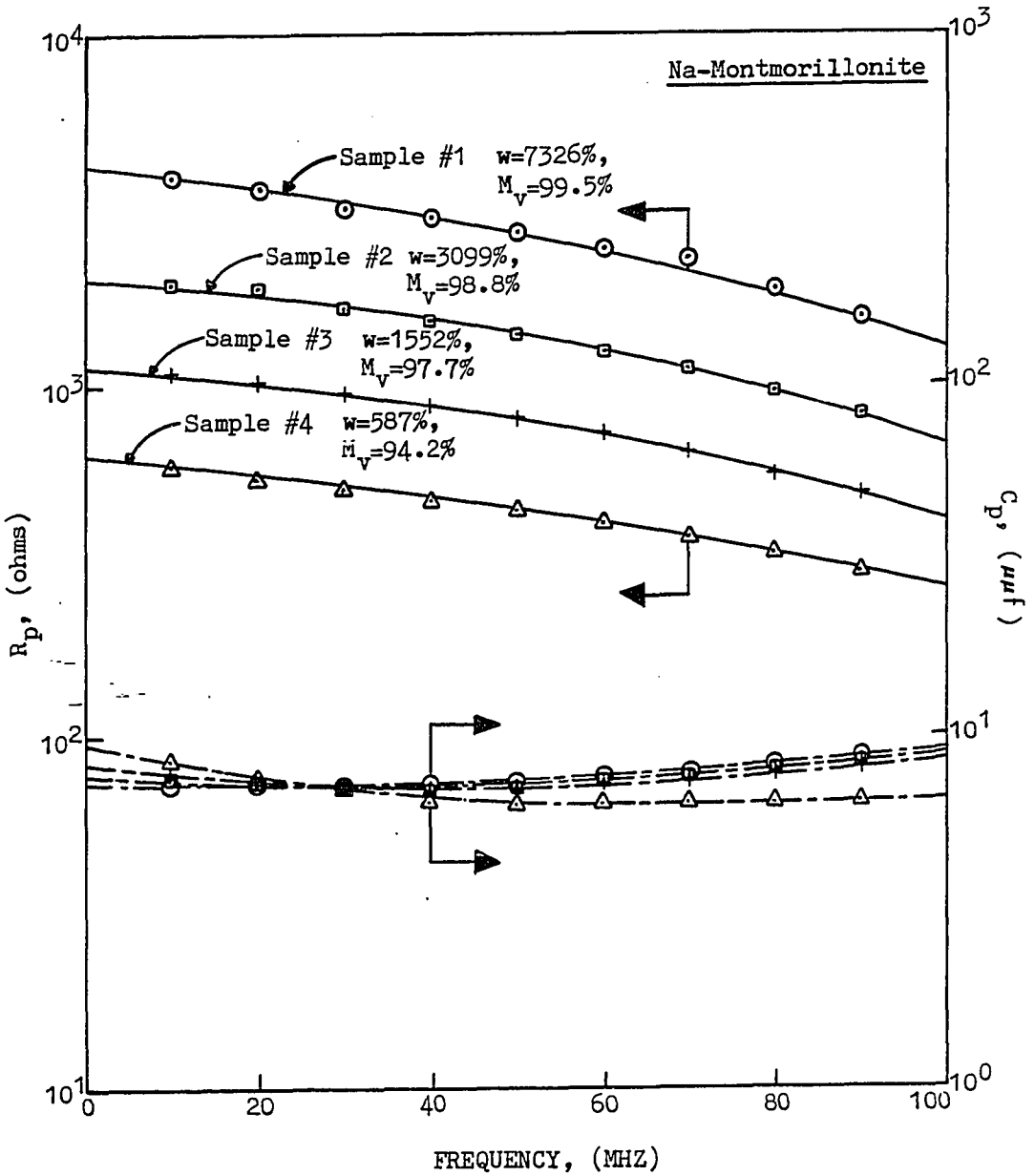

Figure 4. RX-meter 250-A readings for Na-montmorillinite samples; parallel resistance (R_p) and parallel capacitance (C_p)

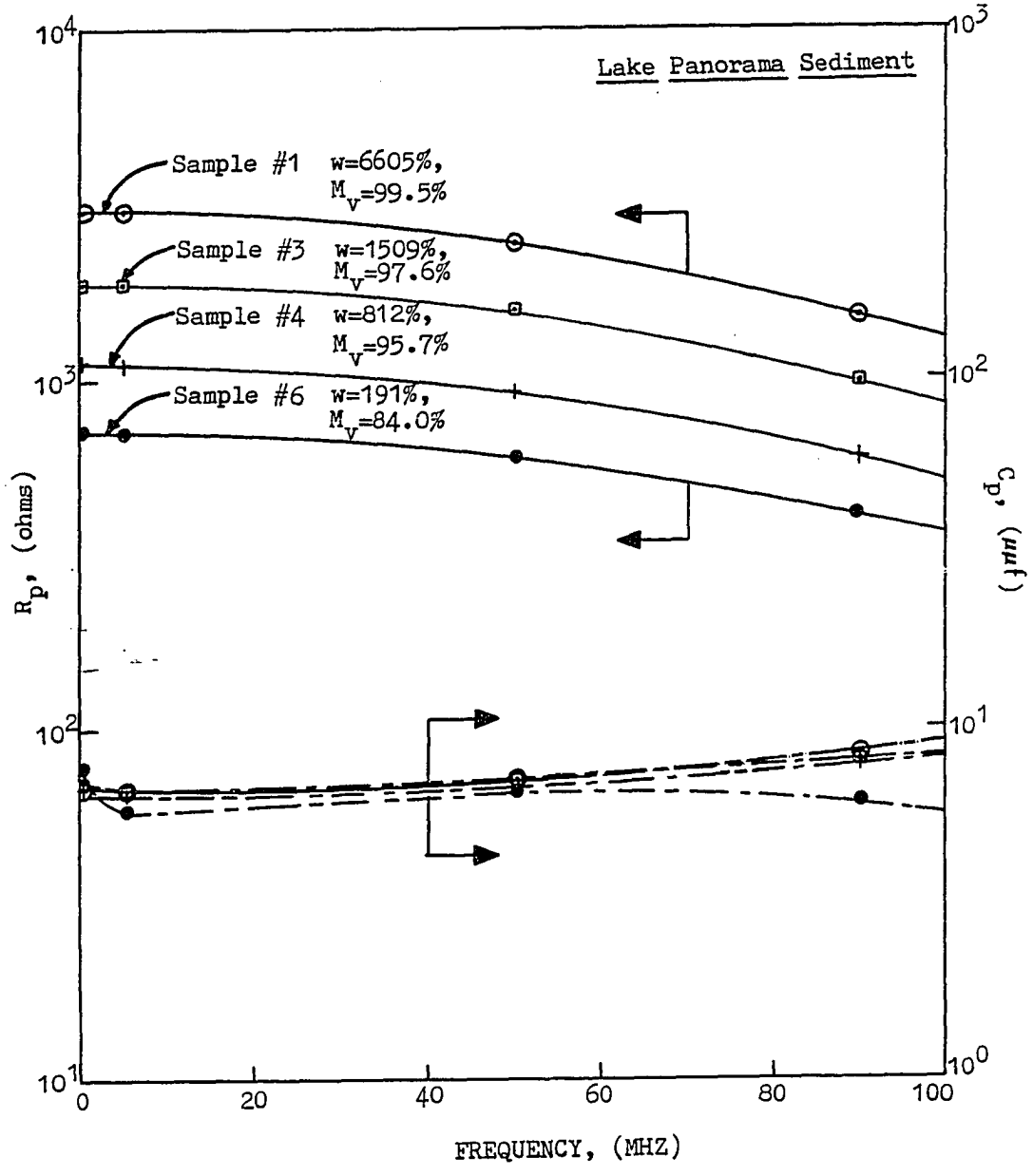

Figure 5. RX-meter 250-A readings for Lake Panorama sediment samples; parallel resistance (R_p) and parallel capacitance (C_p)

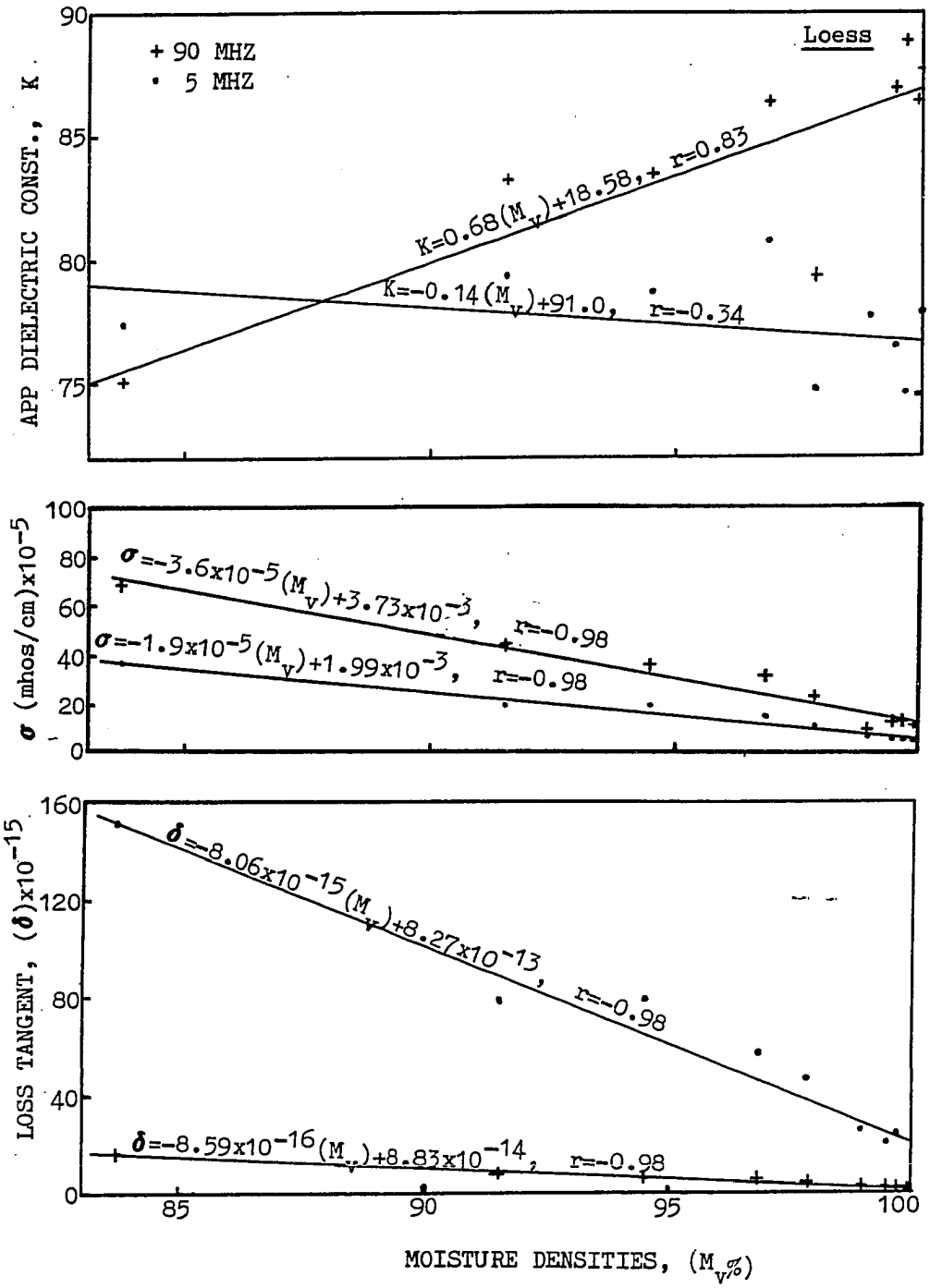

Figure 6. Variation of apparent electrical properties versus moisture density for loess at 5 MHZ and 90 MHZ

computations required to attain the values. Also, it would be difficult to develop a sedimentation column instrument capable of taking readings at two different capacitor gaps, as is required, without disrupting the sedimentation process. That is why relative values are also compared with changes in moisture.

Moisture content, w, was used in plotting the relationship with relative values rather than moisture density; because w versus the relative dielectric constant and relative conductivity results in smooth log-log curves. Figure 7 shows the relationship between the relative dielectric constant and moisture content. It can be observed that there is little increase in the relative dielectric constant with moisture content. Whereas, the relationship between the relative conductivity and moisture content is a smooth curve as shown in Figure 8. The curves are results of the tests at a frequency of 50 MHZ, but similar relationships were observed at all frequencies measured.

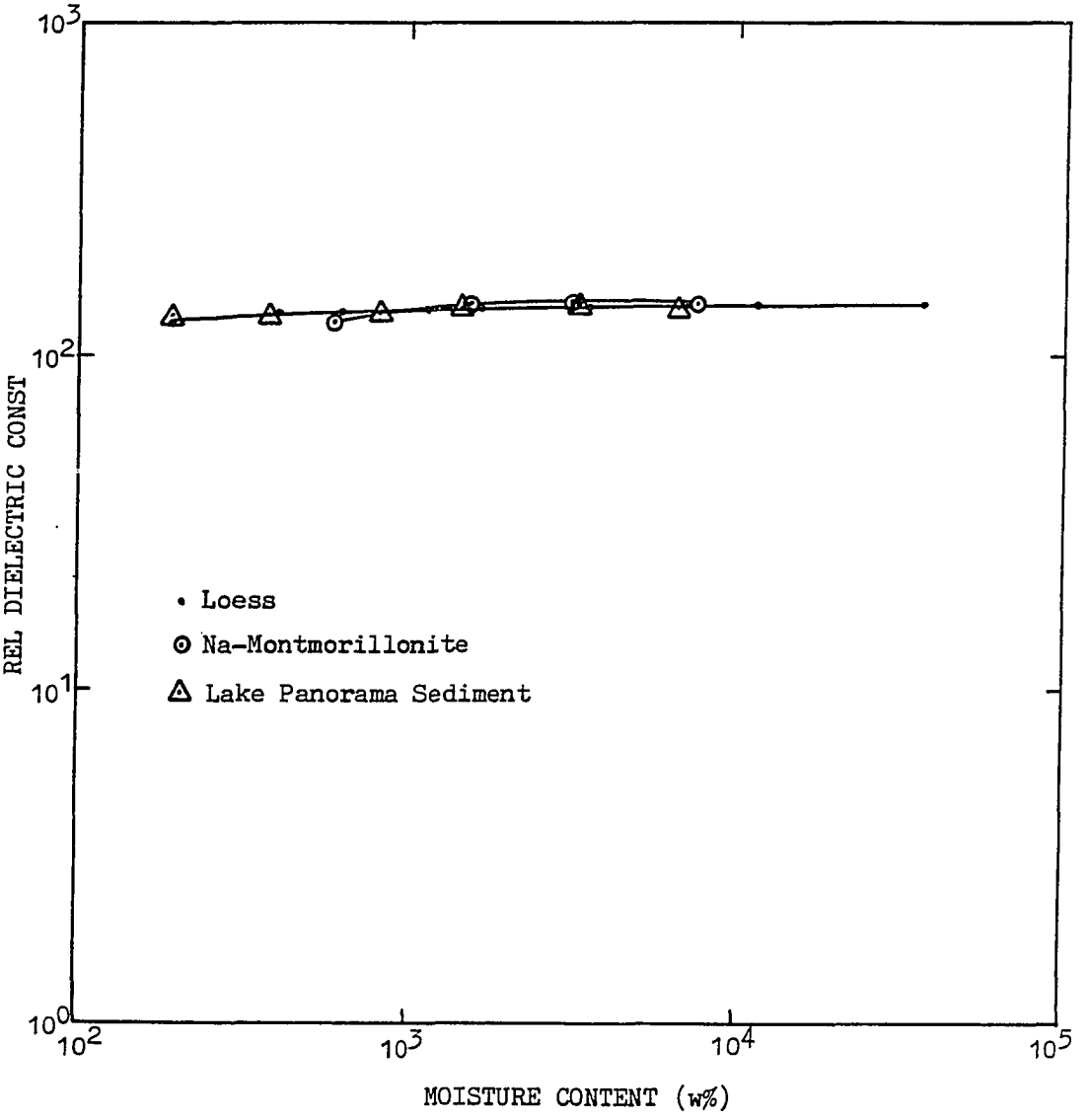

Figure 7. Moisture content versus relative dielectric constant

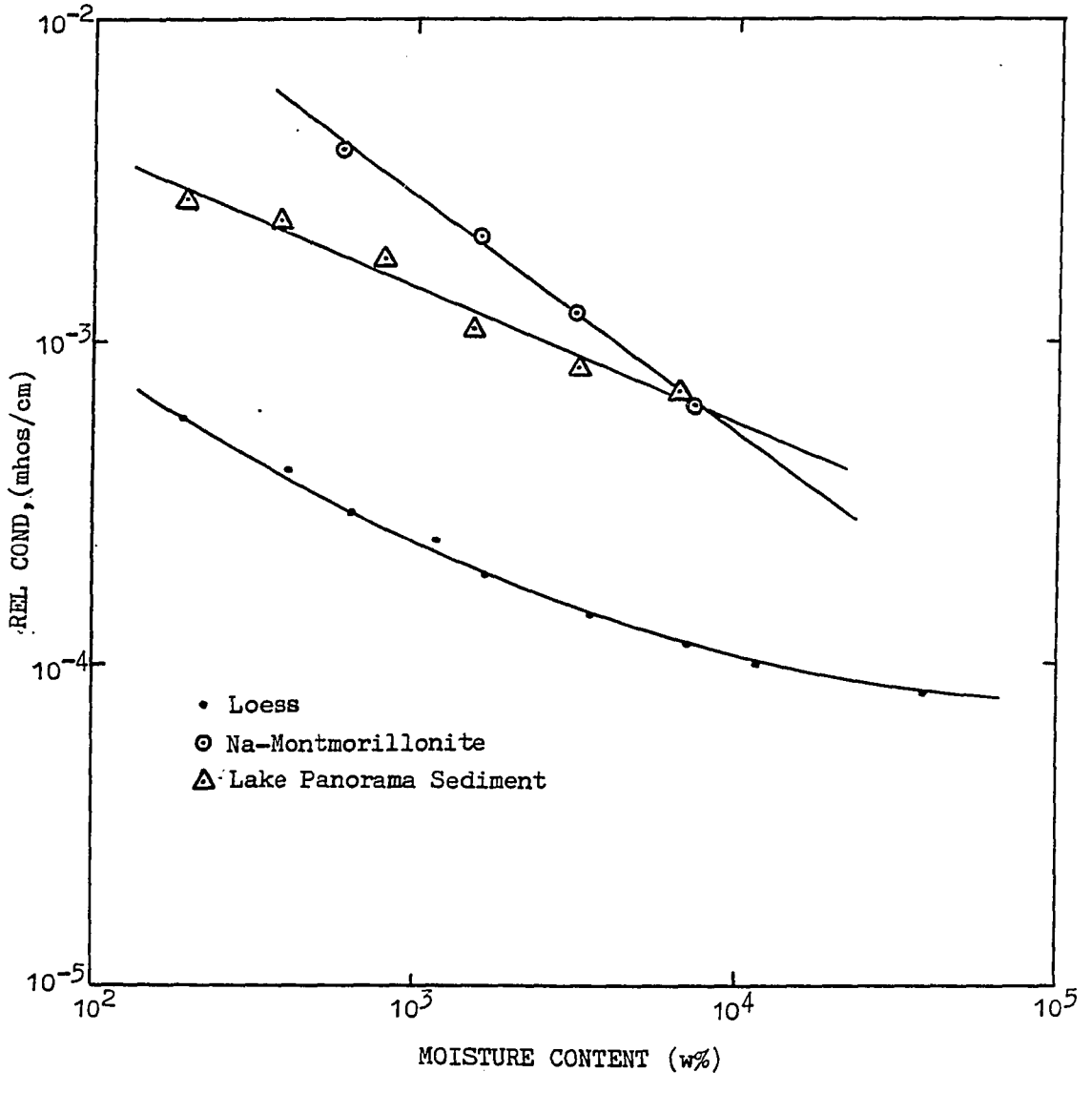

Figure 8. Moisture content versus relative conductivity

CONCLUSIONS

The relative conductivity appears adequate for determining moisture content. The advantages to this approach are:

1. Fewer measurements are required. The apparent value measurements require two different capacitor gaps for evaluation which would make a sedimentation column design more difficult, and
2. Computations are not nearly as complicated for the relative values.

It would be advisable to continue investigations of dielectric constant. The dielectric constant, as previously mentioned, changes with polarization. In the sedimentation process, there is continual change in flocculant structure. At a given time in a sedimentation column, there are regions of small structural change and regions of large change. It is postulated that these changes in structure would also change the polarization properties of the slurry which in turn would change the dielectric constant value.

The use of electrical properties as a means of determining changes in density with depth is thought to be feasible. As the slurry thickens, the concentration of the clay particles increases at the bottom of a sedimentation column and alters the conductivity of the slurry at that level. The preliminary studies presented here suggest the possibility of developing an instrument for measuring the density changes of a slurry. Such an instrument would be useful in sanitary, mining, and geotechnical engineering.

REFERENCES CITED

Arulanandan, K. and S. S. Smith. 1973. Electrical Dispersion in Relation to Soil Structure. American Society of Civil Engineers, 99(SM12):1113-1131.

Been, K. 1980. Stress Strain Behavior of a Cohexive Soil Deposited Under Water. Ph.D. Dissertation. University of Oxford, United Kingdom.

Gaudin, A. M. and M. C. Fuerstenau. 1962. Experimental and Mathematical Model of Thickening. American Institute of Mining Engineers Transactions 223:122-129.

Lin, T. W. 1983. Sedimentation and Self Weight Consolidation of Dredge Spoil. Ph.D. Dissertation. Iowa State University, Ames, Iowa.

Lundien, J. R. 1971. Terrain Analysis by Electromagnetic Means. U.S. Army Engineer Waterways Experiment Station, CE, Vicksburg, Miss., Technical Report 3-727.

Sachs, S. B. and K. S. Spiegler. 1964. Radio Frequency Measurements of Porous Conductive Plugs. Ion-Exchange Resin-Solution Systems. Journal of Physical Chemistry 68(5):2626-2635.

Selig, E. T. and S. Mansukhani. 1975. Relationship of Soil Moisture to Dielectric Property. American Society of Engineers 101(678):755-770.

Smith, S. S. and K. Arulanandan. 1981. Relationship of Electrical Dispersion to Soil Properties. American Society of Civil Engineers 107(GT5):591-604.

Smyth, C. P. 1955. Dielectric Behavior and Structure. McGraw-Hill Book Company, Inc., New York, NY.

Thomas, M. A. 1966. In-Situ Measurements of Moisture in Soil and Similar Substance by Fringe Capacitance. Journal of Scientific Instrumentation 143:21-27.

Wobschall, D. 1977. A Theory of the Complex Dielectric Permittivity of Soil Containing Water: The Semidisperse Model. IEEE Transactions Geoscience Electric GE-15(1):49-58.

GENERAL SUMMARY

The proposed phenomenological process of settling and the model used to predict this settling were found to be reasonable in comparison to the actual settling data taken from the literature. The data used for fitting the model were unique in that they had been carried out using an x-ray transviewer. This testing technique provided the unique boundary information at the base of the slurry essential for running the model. It was therefore noted that for further development of the model it will require greater understanding of the void ratio changes at the base of the slurry. An instrument capable of determining changes in density in a settling slurry would facilitate in the development of this model. The preliminary studies on electrical properties of slurry was carried out for determining the feasibility of using the electrical properties for this purpose.

In addition to this, a simple empirical approach power curve fitting method was found to be adequate for determining settlement of slurries for extended periods of time. The more difficult methods do not appear necessary. It was also noted that by plotting the change in average concentration versus time on a log-log scale it tends to normalize the results onto one line.

Recommendations for Future Study

The success of numerical evaluation of the new model, and in particular, the modeling of the density step propagation is very dependent on the numerical technique itself. Therefore, one of the

primary objectives of future study should involve an evaluation of numerical techniques. The finite element technique is generally accepted as better at modeling discontinuities than finite difference method but the finite element method developed by Wang and Anderson (1982) can surely be improved upon. Possible improvements are as follows: 1) density gradients may be introduced at the lower boundary, 2) the numerical evaluation of the density step may be improved, and 3) source and sink terms may be incorporated for continuous thickener design.

The other necessary area of further research is the development of an economical instrument for determining density changes beneath the solid-liquid interface. Electrical properties have been suggested as the potential means for accomplishing this goal. Once an instrument is developed for this purpose, that does not disturb the system, a better understanding of density changes may become possible.

LITERATURE CITED

Aruanandan, K. and S. S. Smith. 1973. Electrical Dispersion in Relation to Soil Structure. American Society of Civil Engineers, 99(SM12):1113-1131.

Been, K. 1980. Stress Strain Behavior of a Cohesive Soil Deposited Under Water. Ph.D. Dissertation. University of Oxford, United Kingdom.

Been, K. and G. C. Sills. 1981. Self-Weight Consolidation of Soft Soils: An Experimental and Theoretical Study. Geotechnique 31(4):519-535.

Coe, H. S. and G. H. Clevenger. 1916. Methods for Determining the Capacities of Slime-Settling Tanks. American Institute of Mining Engineers Transactions 55(9):356-384.

Coulson, J. M. and J. F. Richardson. 1955. Chemical Engineering. Vol. 2. McGraw-Hill, Inc., New York, NY.

Dell, C. C. and M. B. Kaynar. 1968. Channeling in Flocculated Suspensions. Filtration and Separation 5:323-327.

Dick, R. I. and B. B. Ewing. 1967. Evaluation of Activated Sludge Thickening Theories. American Society of Civil Engineers 93:(SA4):9-29.

Fitch, B. 1962. Sedimentation Process Fundamentals. American Institute of Mining Engineers Transactions 223:129-137.

Fuerstenau, M. C. 1960. The Mechanism of Thickening Kaolin Suspensions. Ph.D. Dissertation. Massachusetts Institute of Technology, Cambridge, Mass.

Gaudin, A. M. and M. C. Fuerstenau. 1962. Experimental and Mathematical Model of Thickening. American Institute of Mining Engineers Transactions 223:122-129.

Gaudin, A. M., M. C. Fuerstenau, and S. R. Mitchell. 1959. Effect of Pulp Depth and Initial Pulp Density in Batch Thickening. American Institute of Mining Engineers Transactions 214:613-616.

Gibson, R. E., G. L. England, and M. J. L. Hussey. 1967. The Theory of One-Dimensional Consolidation of Saturated Clays. Geotechnique 17(3):261-273.

Kynch, C. J. 1952. A Theory of Sedimentation. Faraday Society Transactions 48:166-176.

Lawler, D. F., P. C. Singer, and C. R. O'Melia. 1982. Particle Behavior in Gravity Thickening. Journal of Water Pollution Control Federation 54(10):1388-1400.

Lee, K. and G. C. Sills. 1981. The Consolidation of a Soil Stratum, Including Self-Weight Effects and Large Strains. International Journal for Numerical and Analytical Methods in Geomechanics 5:405-428.

Lin, T. W. 1983. Sedimentation and Self Weight Consolidation of Dredge Spoil. Ph.D. Dissertation. Iowa State University, Ames, Iowa.

Lin, T. W. and R. A. Lohnes. 1984. Sedimentation and Self Weight Consolidation of Dredge Spoil. ASCE Special Publication on Sedimentation/Consolidation Models, pp. 464-480.

Lundien, J. R. 1971. Terrain Analysis by Electromagnetic Means. U.S. Army Engineer Waterways Experiment Station, CE, Vicksburg, Miss., Technical Report 3-727.

Michaels, A. S. and J. C. Bolger. 1962. Settling Rates and Sediment Volumes of Flocculated Kaolin Suspensions. Industrial and Engineering Chemistry Fundamentals 1:24-33.

Mitchell, J. K. 1976. Fundamentals of Soil Behavior. John Wiley and Sons, Inc., New York, NY.

Montgomery, R. L. 1978. Methodology for Design of Fine-Grained Dredged Material Containment Areas for Solids Retention. U.S. Army Engineer Waterways Experiment Station, CE, Vicksburg, Miss., Technical Report D-78-56.

Pusch, R. 1970. Microstructural Changes in Soft Quick Clay at Failure. Canadian Geotechnical Journal 7(1):1-7.

Sachs, S. B. and K. S. Spiegler. 1964. Radiofrequency Measurements of Porous Conductive Plugs. Ion-exchange Resin-solution systems. Journal of Physical Chemistry 68(5):2626-2635.

Samarasinghe, M. A., Y. N. Huang, and V. P. Drnevich. 1982. Permeability and Consolidation of Normally Consolidated Soils. American Society of Civil Engineers 108(GT6):835-850.

Schiffman, R. L., V. Pane, and R. E. Gibson. 1984. The Theory of One-Dimensional Consolidation of Saturated Clays. ASCE Special Publication on Sedimentation/Consolidation Models, pp. 1-29.

Selig, E. T. and S. Mansukhani. 1975. Relationship of Soil Moisture to Dielectric Property. American Society of Engineers 101(GT8):755-770.

Smith, S. S. and K. Arulanandan. 1981. Relationship of Electrical Dispersion to Soil Properties. American Society of Civil Engineers, 107(GT5):591-604.

Smyth, C. P. 1955. Dielectric Behavior and Structure. McGraw-Hill Book Company, Inc., New York, NY.

Taylor, D. W. 1948. Fundamentals of Soil Mechanics. John Wiley and Sons, Inc., New York, NY.

Thomas, M. A. 1966. In-Situ Measurements of Moisture in Soil and Similar Substance by Fringe Capacitance. Journal of Scientific Instruments 43:21-27.

Vande Steeg, J. 1984. Professional Engineer, Shive-Hattery Engineers, Des Moines Iowa. Written Communication. March 21, 1984.

Vesilind, P. E. 1979. Treatment and Disposal of Wastewater Sludges. Ann Arbor, Mich., Ann Arbor Science Publishers, Inc.

Walsh, J. E. and S. M. Bemben. 1981. Containment Area Design for Dredged Lake Materials. Proceedings of the ASCE Specialty Conference Water Forum, pp. 332-341.

Wang, H. F. and M. P. Anderson. 1982. Introduction to Groundwater Modeling. W. H. Freeman and Company, San Francisco, California.

Whitham, G. B. 1974. Linear and Nonlinear Wares. John Wiley and Sons, Inc., New York, NY.

Wobschall, D. 1977. A Theory of the Complex Dielectric Permittivity of Soil Containing Water: The Semidisperse Model. IEEE Transactions Geoscience Electronics GE-15(1):49-58.

Yong, R. N. and D. S. Elmonayeri. 1984. Convection-Diffusion Analysis of Sedimentation in Initially Dilute Solids-Suspension. ASCE Special Publication on Sedimentation/Consolidation Models, pp. 260-274.

ACKNOWLEDGEMENTS

The author wishes to express gratitude to Professor R. A. Lohnes for his advice, help, respect, and trust that he has given me in the time I have been under his guidance. I would also like to express my gratitude to Professor T. A. Austin for taking the time to look over the finite element portion of this dissertation and to Professor T. Demirel for his advice in studying the electrical properties of slurries. Thanks are also extended to Professors T. E. Fenton and C. S. Oulman for serving on my committee.

I would also like to acknowledge the Central Iowa Energy Cooperative for funding this research. Without their support, this research would not have been possible. It is not often that a private entity will fund research in such a manner and for that I am truly grateful.

I also acknowledge my wife who deserves more acknowledgement than I have room to give.

APPENDIX A. FINITE ELEMENT THEORY AND PROGRAM

The modified large strain consolidation equation for modeling settling is as follows:

$$C_F \frac{\partial^2 e}{\partial z^2} - 1.6C_{p2} \frac{\partial e}{\partial z} = \frac{\partial e}{\partial t} \tag{1}$$

Wang and Anderson (1982) used a two-dimensional program for solving a one dimensional transport problem, therefore they were required to add a dispersion coefficient in the transverse directon. Their transport equation is as follows:

$$D_L \frac{\partial^2 c}{\partial x^2} + D_T \frac{\partial^2 c}{\partial y^2} - \bar{v}_x \frac{\partial c}{\partial x} = \frac{\partial c}{\partial t} \tag{2}$$

The transverse dispersion coefficient is immaterial for this one-dimensional problem but is inserted because the program is for two-dimensional problems. The form of the large strain consolidation equation used in this program is as follows:

$$C_T \frac{\partial^2 e}{\partial y^2} + C_F \frac{\partial^2 e}{\partial z^2} - 1.6C_{p2} \frac{\partial e}{\partial z} = \frac{\partial e}{\partial t} \tag{3}$$

Wang and Anderson (1982) applied the Galerkin method for four-node rectangular elements. The residuals of the trial solution $\hat{e}$, weighted by the nodal basis functions $N_L(z,y)$, are set to zero;

$$\iint_D \left(C_T \frac{\partial^2 \hat{e}}{\partial y^2} + C_F \frac{\partial^2 \hat{e}}{\partial z^2} - 1.6C_{p2} \frac{\partial \hat{e}}{\partial z} - \frac{\partial \hat{e}}{\partial t}\right) N_L(z,y)\,dz\,dy = 0 \tag{4}$$

Where L=1,2, ..., NNODE. The trial solution within an element ijmn is an interpolation of the nodal values;

$$\hat{e}^c(z,y,t) = N_i^c(z,y)e_i(t) + N_j^c(z,y)e_j(t) + N_m^c(z,y)e_m(t) + N_n^c(z,y)e_n(t) \tag{5}$$

Where the element nodal basis functions $N_L^c(z,y)$ are defined as follows:

$$N_i^c(z,y) = 1/4(1 - z/a)(1 - y/b)$$
$$N_j^c(z.y) = 1/4(1 + z/a)(1 + y/b)$$
$$N_m^c(z,y) = 1/4(1 + z/a)(1 + y/b)$$
$$N_n^c(z,y) = 1/4(1 - z/a)(1 + y/b)$$

and where:

$$2a = z_j - z_i = z_m - z_n$$
$$2b = y_n - y_i = y_m - y_j \quad .$$

See Figure 1 for mesh coordinate system.

The second spatial derivative terms are integrated by parts and the integration over the domain is done element by element.

$$\sum_C \left[\iint_c \left(C_T \frac{\partial \hat{e}^c}{\partial y} \frac{\partial N_L}{\partial y} + C_F \frac{\partial \hat{e}^c}{\partial z} \frac{\partial N_L}{\partial z} + 1.6\ C_{p2} \frac{\partial \hat{e}^c}{\partial z} N_L \right. \right.$$

$$\left. \left. + \frac{\partial \hat{e}}{\partial t} N_L \right) dzdy \right] = \int_T \left(C_T \frac{\partial \hat{e}^c}{\partial y} n_y + C_F \frac{\partial \hat{e}}{\partial z} N_z \right) N_L d\sigma \tag{7}$$

Where L=1,2, ..., NNODE .

The system of equations represented by Equation (7) can be written in matrix notation in the form:

$$[G]\{E\} + [U]\{E\} + [P]\left\{\frac{\partial e}{\partial t}\right\} = \{f\} \tag{8}$$

Where {E} is the column matrix of nodal void ratio and { e/ t} is the column matrix of the time derivative. [G], [U], and [P] are square coefficient matrices corresponding to individual terms in the integral on the left-hand side of Equation (7). The [G] and [P] matrices in Equation (8) have element matrix entries which are:

$$G^c_{L,i} = \int_{-a}^{a}\int_{-b}^{b} \left(C_T \frac{\partial N^c_i}{\partial y}\frac{\partial N^c_L}{\partial y} + C_F \frac{\partial N^c_i}{\partial z}\frac{\partial N^c_L}{\partial z}\right) dzdy \tag{9}$$

$$P^c_{L,i} = \int_{-a}^{a}\int_{-b}^{b} N^c_i N^e_L \, dzdy \quad . \tag{10}$$

The matrix [U] derives from the advective term $1.6\ C_{p2}(\partial \hat{e}^c/\partial z)N_L$ in the integrand of Equation (7). Taking the z derivative of Equation (5) yields:

$$\frac{\partial \hat{e}^c}{\partial z} = \frac{\partial N^c_j}{\partial z} e_i + \frac{\partial N^c_j}{\partial z} e_i + \frac{\partial N^c_m}{\partial z} e_m + \frac{\partial N^c_n}{\partial z} e_n \tag{11}$$

Therefore, the coefficient which multiplies e_i is

$$U^c_{L,i} = 1.6C_{p2} \int_{-a}^{a}\int_{-b}^{b} \frac{\partial N^c_i}{\partial z} N_L{}^c \, dzdy \tag{12}$$

Similarly, the remaining element matrix terms are:

$$U^c_{L,j} = 1.6C_{p2} \int_{-a}^{a} \int_{-b}^{b} \frac{\partial N^c_j}{\partial z_c} N_L{}^c \, dzdy$$

$$U^c_{L,m} = 1.6C_{p2} \int_{-a}^{a} \int_{-b}^{b} \frac{\partial N^c_m}{\partial z_c} N_L{}^c \, dzdy$$

$$U^c_{L,n} = 1.6C_{p2} \int_{-a}^{a} \int_{-b}^{b} \frac{\partial N^c_m}{\partial z} N_L{}^c \, dzdy$$

The evaluation of the integrals is done by Gaussian quadrature. Numerical integration by Gaussian quadrature is easy to code in a computer. The double-integral generalization for a second-degree polynomial $g(\xi,\eta)$ is

$$\int_{-1}^{1} \int_{-1}^{1} g(\xi,\eta)d\xi d = g(\xi,\eta_1) + g(\xi_2,\eta_1) + g(\xi_1,\eta_2) + g(\xi_2,\eta_2) \, .$$

Where the four Gauss points are defined by $\eta_1 = -1/\sqrt{3}$, $\eta_2 = 1/\sqrt{3}$, $\eta_1 = -1/\sqrt{3}$, and $\eta_2 = 1/\sqrt{3}$. All the weighting coefficients are equal to one.

$$\xi = \frac{z}{a} \quad \text{and} \quad \eta = \frac{y}{b} \, . \tag{14}$$

Then, $dz = a \cdot d\xi$ and $dy = b \cdot d\xi$. The limits of integration become -1 to 1 and the interpolation functions in (ξ,η) coordinates are

$$\tilde{N}^c_i(\xi,\eta) = 1/4(1 - \xi)(1 - \eta)$$

$$\tilde{N}^c_j(\xi,\eta) = 1/4(1 + \xi)(1 - \eta)$$

$$\tilde{N}_m^c(\xi,\eta) = 1/4(1+\xi)(1+\eta)$$

$$\tilde{N}_n^c(\xi,\eta) = 1/4(1-\xi)(1+\eta)$$

In summary, the integrals transform according to

$$\int_{-a}^{a}\int_{-b}^{b} g(z,y)\,dzdy = ab\int_{-1}^{1}\int_{-1}^{1} \tilde{g}(\xi,\eta)\,d\xi d\eta \quad .$$

Where $\tilde{g}(\xi,\eta)$ is $g(z,y)$ expressed in (ξ,η) coordinates.

The assembly of the global matrices is performed by summation of the element terms. Note that the matrix equation has the form

$$[A]\{e\} + [P]\frac{\partial e}{\partial t} = \{f\} \quad . \tag{16}$$

Where $[A] = [G] + [U]$. The entries of $[G]$ are symmetric in their subscripts. However, the entries to $[U]$ from the advective term are not symmetric in their subscripts. Consequently, we have to store in the computer core coefficients on the entire band. This aspect requires relatively more computer time in solving the equations as compared to the time required for symmetric and banded systems.

The stepping through time of the solution for the nodal void ratios is done by a finite difference approximation of the time derivative for $\{\partial e/\partial t\}$. What is usually called the finite element method of solving this equation is a hybrid of finite element and finite difference concepts.

Finite Element Computer Program

The finite element program to solve the settling problem has required a few modifications of the computer program for solute transport (Wang and Anderson, 1982). The rectangular finite element mesh is used for one-dimensional settling problem. The boundary conditions are

For $t=0$ $e(z,0)= e_1$

$C_F = C_F$

$C_T = C_{p2}$

$C_p = 0$.

For $0 < t < t_1$ $e(0,t)$ = predetermined value

$e(z_t,t)=e_i$

$C_F = C_F$

$C_T = C_{p2}$

$C_p = 0$.

For $t_1 < t$ $e(0,t)$ = predetermined value

$e(z_t,t)=e_u$

$C_F = C_F$

at $e > e_a$ $C_p = C_{p2}$

at $e < e_a$ $C_p = 0$.

See Figure 2 for the boundary conditions of settling. The following pages contain the finite element program to solve one-dimensional settling problem, along with the output.

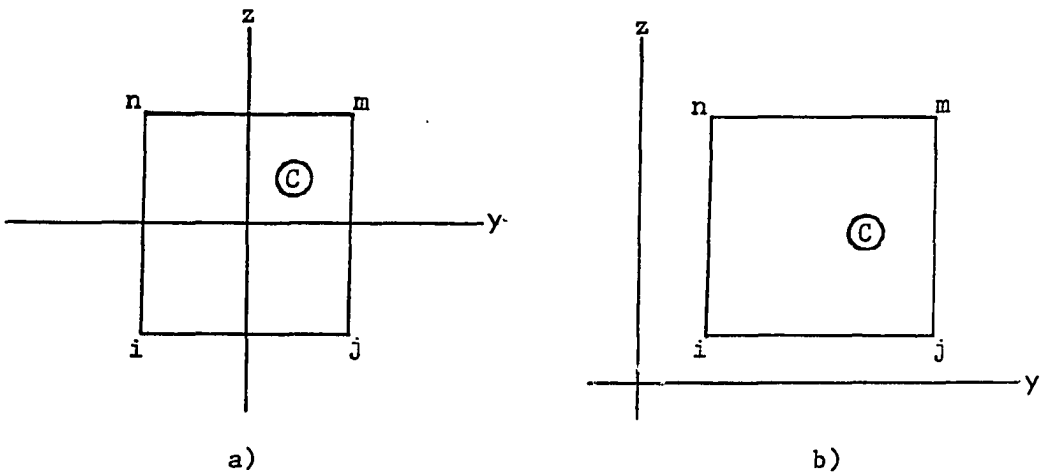

Figure 1. The archetypal rectangular element c
a) in local coordinates; b) in global coordinates

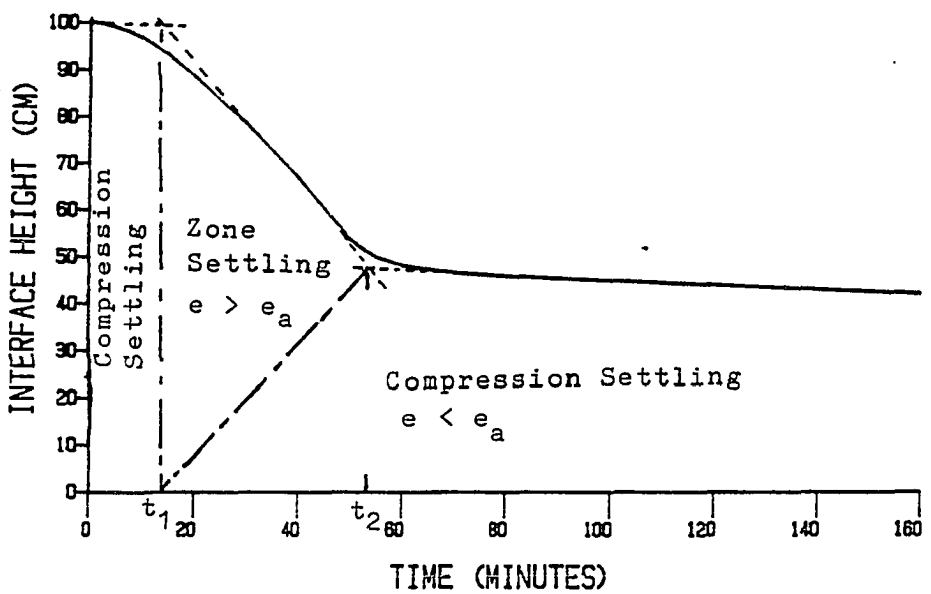

Figure 2. Boundary conditions of settling

```
C     FINITE ELEMENT PROGRAM FOR SEDIMENTATION USING FOUR NODE
C     ELEMENTS.  MODIFIED FROM "INTRODUCTION TO GROUNDWATER"
C     BY WANG AND ANDERSON (1982).
C
C     VARIABLES ARE DEFINED AS FOLLOWS:
C         NS=INTERPOLATION FUNCTIONS
C         NX&NY=COORDINATE DERIVATIVES
C         EOLD=VOID RATIO @ PRESENT TIME
C         ENEW=VOID RATIO AT NEXT TIME STEP
C         G=SQUARE MATRIX FOR CONDUCTANCE TERM
C         P=SQUARE MATRIX FOR STORAGE TERM
C         U=SQUARE MATRIX FOR ADVECTIVE TERM
C         B=THE MATRIX FOR WEIGHT FUNCTION
C         X=THE COORDINATE LOCATION
C         XSI=GAUSS POINTS
C         ETA=GAUSS POINTS
C         NODE=LOCAL NODE NUMBERING SYSTEM
C         EI=INITIAL VOID RATIO
C         E=VOID RATIO @ CONTROL POINTS
C         HI=INITIAL HEIGHT
C         GS=SPECIFIC GRAVITY OF SOIL
C         CF=COEFFICIENT OF CONSOLIDATION
C         CP=COEFFICIENT OF PERMEABILITY
C         UFE=VELOCITY OF ADVECTIVE TERM
C         RHOF=DENSITY OF FLUID
C         RHOS=DENSITY OF SOLID
C         DENS=DENSITY OF FLUID AND SOLID COMBINED
C         NNODE=NUMBER OF NODES
C         NELEM=NO. OF ELEMENTS
C
C
      REAL NS,NX,NY
      DIMENSION EOLD(36),ENEW(36),G(36,36),P(36,36),U(36,36)
      DIMENSION B(36),X(36),Y(36),UFE(36)
      DIMENSION XSI(4),ETA(4),NS(4),NX(4),NY(4),NODE(4)
      DATA XSI/-.57735,.57735,.57735,-.57735/
      DATA ETA/-.57735,-.57735,.57735,.57735/
      READ, EI,HI,GS,TO,ED
      PRINT,  'INITIAL VOID RATIO=',EI
      PRINT,  'INITIAL SLURRY HIEGHT=',HI,'CM'
      PRINT,  'SPECIFIC GRAVITY=',GS
      PRINT,  'TIME OF STRUCTURE COLLAPSE=',TO,'MIN'
      PRINT,  'VOID RATIO AT WHICH DIFFUSION DOMINATES=',ED
      READ,  CP,CF
      PRINT,  'PERMEABILITY COEFFICIENT=',CP
      PRINT,  'COEFFICIENT OF CONSOLIDATION=',CF
C
C     CALCULATE THE VALUE FOR MATERIAL COORDINATES AND DENSITIES
C
      TIME=0.0
      RHOF=9.8
```

```
      RHOS=GS*(RHOF)
      NNODE=36
      NELEM=17
      DZ=HI/((10.0)*(1.0+EI))
C
C     BLOCK#1. GENERATE NODAL COORDINATES AND INITIAL BOUNDARY
C              CONDITIONS.
C
      DO 10 L=1,NNODE,2
      X(L)=FLOAT(L-1)*DZ/2.0
      X(L+1)=X(L)
      Y(L)=DZ
   10 Y(L+1)=0.0
      DO 15 L=1,NNODE
      EOLD(L)=EI
      ENEW(L)=EI
      SET=ENEW(L)
      VALUE=0.0
      IF(SET.GT.0.)VALUE=((SET**2.)*(3.+SET))/((1.0+SET)**3.0)
      UFE(L)=(RHOS-RHOF)*CP*VALUE/RHOF
      DO 15 JJ=1,NNODE
      G(L,JJ)=0
      U(L,JJ)=0
   15 P(L,JJ)=0
C
C     BLOCK#2. CONSTRUCT GLOBAL COEFFICIENT MATRICES
C
      DO 100 K=1,NELEM
C
C     GENERATE NODE NO. OF ELEMENTS
C
      I=2*K
      J=J+2
      M=I+1
      N=I-1
      VX=(UFE(I)+UFE(J))/2.0
      IF(TO .GT. TIME)VX=0.0
      DY=VX
      NODE(1)=I
      NODE(2)=J
      NODE(3)=M
      NODE(4)=N
      AA=ABS(X(J)-X(I))/2.0
      BB=ABS(Y(N)-Y(I))/2.0
      DO 40 KK=1,4
      L=NODE(KK)
C
C     GAUSSIAN GUADRATURE
C
      DO 30 IQ=1,4
      NS(1)=.25*(1.0-XSI(IQ))*(1.0-ETA(IQ))
```

```
      NS(2)=.25*(1.0+XSI(IQ))*(1.0-ETA(IQ))
      NS(3)=.25*(1.0+XSI(IQ))*(1.0+ETA(IQ))
      NS(4)=.25*(1.0-XSI(IQ))*(1.0+ETA(IQ))
      NX(1)=-.25*(1.0-ETA(IQ))/AA
      NX(2)=.25*(1.0-ETA(IQ))/AA
      NX(3)=.25*(1.0+ETA(IQ))/AA
      NX(4)=-.25*(1.0+ETA(IQ))/AA
      NY(1)=-.25*(1.0-XSI(IQ))/BB
      NY(2)=-.25*(1.0+XSI(IQ))/BB
      NY(3)=.25*(1.0+XSI(IQ))/BB
      NY(4)=.25*(1.0-XSI(IQ))/BB
      G(L,I)=G(L,I)+(CF*NX(1)*NX(KK)+DY*NY(1)*NY(KK))*AA*BB
      G(L,J)=G(L,J)+(CF*NX(2)*NX(KK)+DY*NY(2)*NY(KK))*AA*BB
      G(L,M)=G(L,M)+(CF*NX(3)*NX(KK)+DY*NY(3)*NY(KK))*AA*BB
      G(L,N)=G(L,N)+(CF*NX(4)*NX(KK)+DY*NY(4)*NY(KK))*AA*BB
      U(L,I)=U(L,I)+VX*NX(1)*NS(KK)*AA*BB
      U(L,I)=U(L,J)+VX*NX(2)*NS(KK)*AA*BB
      U(L,M)=U(L,M)+VX*NX(3)*NS(KK)*AA*BB
      U(L,N)=U(L,N)+VX*NX(4)*NS(KK)*AA*BB
      P(L,I)=P(L,I)+NS(1)*NS(KK)*AA*BB
      P(L,J)=P(L,J)+NS(2)*NS(KK)*AA*BB
      P(L,M)=P(L,M)+NS(3)*NS(KK)*AA*BB
      P(L,N)=P(L,N)+NS(4)*NS(KK)*AA*BB
   30 CONTINUE
   40 CONTINUE
  100 CONTINUE
C
C     CONSTRUCT B-MATRIX FOR EACH TIME STEP
C
      PRINT 120
  120 FORMAT(1H1,26X,'CONCENTRATION',32X,'TIME',//)
      DT=5.
      KOUNT=1
      KPRINT=2
      TIME=DT
      DO 500 NSTEP=1,32
      READ, EN
      ENEW(1)=EN
      ENEW(2)=ENEW(1)
      DO 150 L=1,NNODE
      B(L)=0
      DO 150 JJ=1,NNODE
      B(L)=B(L)+P(L,JJ)*EOLD(JJ)/DT
  150 CONTINUE
  200 AMAX=0.0
      DO 400 L=1,NNODE
      IF((L.EQ.1).OR.(L.EQ.2).OR.(L.EQ.35).OR.(L.EQ.36))GO TO 400
      OLDVAL=ENEW(L)
      SUM=0.0
      DO 300 JJ=1,NNODE
      IF(JJ.EQ.L)GO TO 300
```

```
      SUM=SUM+(G(L,JJ)+U(L,JJ)+P(L,JJ)/DT)*ENEW(JJ)
  300 CONTINUE
      ENEW(L)=(-SUM+B(L))/(G(L,L)+U(L,L)+P(L,L)/DT)
      ERR=ABS(OLDVAL-ENEW(L))
      IF(ERR.GT.AMAX)AMAX=ERR
  400 CONTINUE
      IF(AMAX.GT.0.01)GO TO 200
      DO 450 L=1,NNODE
      EOLD(L)=ENEW(L)
      SET=ENEW(L)
      VALUE=0.0
      IF(SET.GT.0.)VALUE=((SET**2.)*3.+SET))/((1.+SET)**3.)
      UFE(L)=(RHOS-RHOF)*CP*VALUE/RHOF
      IF(ED.GT.EOLD(L))UFE(L)=0.0
      DO 450 JJ=1,NNODE
         G(L,JJ)=0.0
         U(L,JJ)=0.0
  450 CONTINUE
C
C     GENERATE VALUES FOR NEXT TIME STEP
C
      DO 480 K=1,NELEM
       I=2*K
       J=I+2
       M=I+1
       N=I-1
      VX=(UFE(I)+UFE(J))/2.0
      IF(TO.GT.TIME)VX=0.0
      DY=VX
      NODE(1)=I
      NODE(2)=J
      NODE(3)=M
      NODE(4)=N
      DO 470 KK=1,4
      L=NODE(KK)
      DO 460 IQ=1,4
      NS(1)=.25*(1.0-XSI(IQ))*(1.0-ETA(IQ))
      NS(2)=.25*(1.0+XSI(IQ))*(1.0-ETA(IQ))
      NS(3)=.25*(1.0+XSI(IQ))*(1.0+ETA(IQ))
      NS(4)=.25*(1.0-XSI(IQ))*(1.0+ETA(IQ))
      NX(1)=-.25*(1.0-ETA(IQ))/AA
      NX(2)=.25*(1.0-ETA(IQ))/AA
      NX(3)=.25*(1.0+ETA(IQ))/AA
      NX(4)=-.25*(1.0+ETA(IQ))/AA
      NY(1)=-.25*(1.0-XSI(IQ))/BB
      NY(2)=-.25*(1.0+XSI(IQ))/BB
      NY(3)=.25*(1.0*XSI(IQ))/BB
      NY(4)=.25*(1.0-XSI(IQ))/BB
      G(L,I)=G(L,I)+(CF*NX(1)*NX(KK)+DY*NY(1)*NY(KK))*AA*BB
      G(L,J)=G(L,J)+(CF*NX(2)*NX(KK)+DY*NY(2)*NY(KK))*AA*BB
      G(L,M)=G(L,M)+(CF*NX(3)*NX(KK)+DY*NY(3)*NY(KK))*AA*BB
```

```
      G(L,N)=G(L,N)+(CF*NX(4)*NX(KK)+DY*NY(4)*NY(KK))*AA*BB
      U(L,I)=U(L,I)+VX*NX(1)*NS(KK)*AA*BB
      U(L,J)=U(L,J)+VX*NX(2)*NS(KK)*AA*BB
      U(L,M)=U(L,M)+VX*NX(3)*NS(KK)*AA*BB
      U(L,N)=U(L,N)+VX*NX(4)*NS(KK)*AA*BB
  460 CONTINUE
  470 CONTINUE
  480 CONTINUE
      IF(KOUNT.NE.KPRINT)GO TO 490
      PRINT 401,TIME
  401 FORMAT(1X,'TIME=',1F10.2)
      PRINT 402
  402 FORMAT(1X,'ELEMENT',6X,'LOCATION(CM)',8X,'VOID RATIO',5X,
     +'DENSITY',/)
      X(1)=0.0
      DX=1.0
      DO 485 L=1,22,2
      IF(L.EQ.1)GO TO 483
      I=L-2
      DX=DZ*(1.0+(ENEW(L)+ENEW(I))/2.0)
      X(L)=X(I)+DX
  483 RHOT=RHOF*((ENEW(L)+GS)/(1.0+ENEW(L)))
      PRINT 482, L,X(L),ENEW(L),RHOT
  482 FORMAT(4X,I4,6X,F11.3,10X,F9.3,6X,F6.2)
  485 CONTINUE
      IF(KOUNT.NE.KPRINT)GO TO 490
      KOUNT=0
  490 TIME=TIME+DT
      KOUNT=KOUNT+1
  500 CONTINUE
      STOP
      END
```

SAMPLE PRINTOUT

TIME= 10.00 MINUTES

ELEMENT	LOCATION(CM)	VOID RATIO	DENSITY
1	0.000	13.600	10.87
3	7.655	17.805	10.63
5	16.692	19.634	10.56
7	26.317	20.370	10.53
9	36.175	20.653	10.52
11	46.123	20.759	10.52
13	56.104	20.798	10.52
15	66.097	20.812	10.52
17	76.094	20.817	10.52
19	86.093	20.819	10.52
21	96.093	20.820	10.52

APPENDIX B. SETTLING TEST DATA

Test N-1

C_i = 75.3 g/l (C_i = initial concentration)

H_i = 179.7 cm (H_i = initial height)

Time (hrs)	Interface Hght (cm)
1.33	88.8
1.42	86.9
1.50	85.2
1.67	82.3
1.83	79.5
2.00	76.7
2.50	68.6
3.50	59.1
3.75	54.0
4.00	52.1
4.50	49.3
5.00	47.0

Test N-2

C_i = 101 g/l

H_i = 179.7 cm

Time (Hrs)		Interface Hgt (cm)	
1.17		125.5	
1.25		123.8	
1.33		122.2	
1.50		118.9	
1.67		116.1	
1.75		114.3	
1.83		113.0	
2.00		110.0	
3.00		93.7	
3.50		86.9	
4.00		80.6	
4.50		75.6	
5.00		71.1	
5.50		67.1	
6.00	Time	64.0	Ave. Conc.
6.50	(days)	61.2	(g/l)
7.16	0.30	58.7	309.2

N-3

C_i = 147 g/l

H_i = 179.7 cm

Time (hrs)	Interface Hght (cm)
0.17	176.8
0.25	175.5
0.33	174.4
0.50	172.0
0.75	168.4
1.00	165.1
1.50	158.8
2.33	148.3
3.00	140.5
3.50	134.9
4.00	129.5
4.50	124.2
5.50	114.0
6.00	109.5
7.58	96.5
8.58	89.5
9.50	83.6
10.50	78.7
11.67	76.7
12.67	75.6
14.00	74.3
22.58	69.9
34.0	65.3
45.5	62.7
56.0	60.6

Time (days)	Ave. Conc. (g/l)
0.49	344.4
0.53	349.6
0.58	355.5
0.94	378.2
1.42	404.7
1.90	421.0
2.33	435.7

Test N-4

C_i = 191.5 g/l

H_i = 180.3

Time (hrs)	Interface Hght (cm)
0.17	178.4
0.33	177.3
0.50	176.3
0.75	174.9
1.00	173.2
1.50	169.8
2.00	166.0
3.00	158.0
4.00	150.5
5.00	143.8
6.00	137.2
7.00	131.1
8.00	125.0
9.75	114.9
10.5	110.7
12.3	99.6
13.3	93.9
14.1	90.5
15.0	89.2
16.67	87.6
25.50	83.2
30.0	81.5
32.8	80.6
38.0	79.4
49.9	76.8
53.0	76.3

Time (Days)	Ave. Conc. (g/l)
0.70	394.1
1.06	415.0
1.25	423.6
1.37	428.4
1.58	434.9
2.08	449.3
2.21	452.3

Test N-5

C_i = 226.5 g/l

H_i = 71.25"

Time (Hrs)	Interface Hght (cm)
0.25	179.1
1.25	178.8
1.75	178.8
2.91	171.2
4.00	162.6
5.00	155.6
6.00	149.2
7.00	143.5
8.25	136.5
9.03	132.3
10.0	127.0
11.0	121.7
12.0	116.2
13.3	109.9
16.0	104.3
17.3	103.0
23.3	99.1
25.6	97.8
30.1	96.0
30.1	96.0
34.6	94.6
46.5	91.7
49.9	90.8
52.1	90.2
58.2	89.0
70.3	86.9

Time (Days)	Ave. Conc. (g/l)
0.97	413.6
1.07	419.1
1.26	427.0
1.26	427.0
1.44	433.3
1.94	447.1
2.08	451.4
2.17	454.6
2.42	460.4
2.93	471.9

Modified Self Weight Consolidation Solution

Test N-3

$$H(t) = 176.8 - 129.0\ (S_m(T'))$$ Equation (3) of Part III

Variables used for solution of $S_m(T')$ are taken from Table 1 of Part III and are as follows:

$$r = 0.22$$

$$C_F = 0.017^2/\text{min} = 157.94\ \text{cm}^2/\text{day}$$

$$T = 0.0818(t)$$

$$t = \text{time in days.}$$

Table B1. Solution of Equation (3) of Part III at various times

Time (days)	T'	$S_m(T')$	H(t) (cm)	C (g/l)
0.5	0.0409	0.22	148.4	178
0.7	0.0573	0.26	143.2	184
1.0	0.0818	0.32	135.5	195
2.0	0.1636	0.45	118.7	223
4.0	0.3272	0.64	94.2	280
10.0	0.8180	0.89	61.9	427
50.0	4.0898	1.00	47.8	553
100.0	8.1896	1.00	47.8	553